



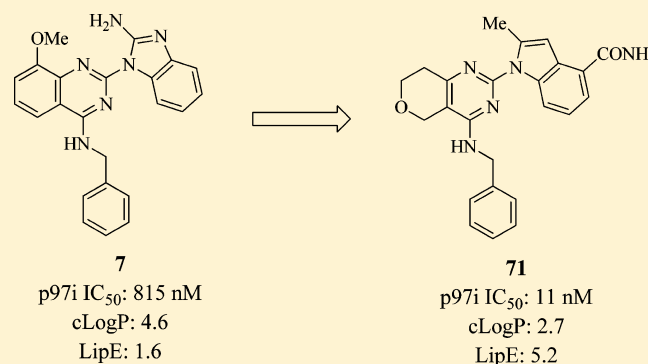
Discovery of a First-in-Class, Potent, Selective, and Orally Bioavailable Inhibitor of the p97 AAA ATPase (CB-5083)

Han-Jie Zhou,* Jinhai Wang, Bing Yao, Steve Wong, Stevan Djakovic, Brajesh Kumar, Julie Rice, Eduardo Valle, Ferdie Soriano, Mary-Kamala Menon, Antonett Madriaga, Szerenke Kiss von Soly, Abhinav Kumar, Francesco Parlati, F. Michael Yakes, Laura Shawver, Ronan Le Moigne, Daniel J. Anderson, Mark Rolfe, and David Wustrow

Cleave Biosciences Inc., 866 Malcom Road, Burlingame, California 94010, United States

S Supporting Information

ABSTRACT: The AAA-ATPase p97 plays vital roles in mechanisms of protein homeostasis, including ubiquitin–proteasome system (UPS) mediated protein degradation, endoplasmic reticulum-associated degradation (ERAD), and autophagy. Herein we describe our lead optimization efforts focused on in vitro potency, ADME, and pharmaceutical properties that led to the discovery of a potent, ATP-competitive, D2-selective, and orally bioavailable p97 inhibitor **71**, CB-5083. Treatment of tumor cells with **71** leads to significant accumulation of markers associated with inhibition of UPS and ERAD functions, which induces irresolvable proteotoxic stress and cell death. In tumor bearing mice, oral administration of **71** causes rapid accumulation of markers of the unfolded protein response (UPR) and subsequently induces apoptosis leading to sustained antitumor activity in in vivo xenograft models of both solid and hematological tumors. **71** has been taken into phase 1 clinical trials in patients with multiple myeloma and solid tumors.



INTRODUCTION

The protein p97 (also called valosin-containing protein (VCP), or CDC48 in yeast) is an abundant AAA+ ATPase associated with a variety of cellular activities.¹ Working together with various cofactors,² p97 is involved in multiple biological processes including protein homeostasis,³ ERAD,⁴ autophagy,⁵ chromatin remodeling,⁶ and Golgi reassembly,⁷ where it supplies the mechanical force required for extracting proteins by hydrolyzing ATP. Under physiological conditions, p97 forms a ring-shaped homohexamer.^{1b,8} The ATPase activity of p97 is crucial for conversion of the potential energy in ATP into mechanical energy via conformational changes in the p97 hexamer. Each p97 protomer consists of three domains: two ATPase domains (D1 and D2) and one N-terminal domain.⁹ The N-terminal domain binds various cofactors that interact with a variety of substrate proteins. The D1 domain has low basal ATPase activity owing in part to a very low off rate of ADP.³ The D2 domain is thought to be responsible for most of the ATPase activity of p97 under physiological conditions.¹⁰ The D2 ATPase region has been shown to have both a higher *K_m* for ATP and a faster hydrolysis of ATP to ADP.¹⁰ Numerous studies have implicated p97's role in promoting ERAD in collaboration with the UPS. For instance, p97 in combination with substrate recruiting cofactors Ufd1 and Np14 extracts misfolded poly-ubiquitinated proteins from the

endoplasmic reticulum (ER) into the cytosol and then delivers them to the proteasome for degradation.¹¹

Expression of p97 is essential to maintain protein homeostasis, especially under stressed conditions. Indeed, siRNA knockdown of p97 causes irresolvable ER stress and activates the UPR, leading to apoptosis via UPS inhibition and activation of caspases.¹² This observation has led to the hypothesis that p97 inhibition (p97i) could preferentially kill those cancer cells that have a high protein synthesis burden. Small molecules that inhibit the ATPase function of p97 could prevent the mechanical action of various p97 containing complexes and therefore inhibit the UPS, activate the UPR, and induce apoptosis. A number of small molecule inhibitors of p97 activity have been previously described.¹³ A high-throughput screening (HTS) campaign for inhibition of p97 ATPase activity followed by hit-to-lead optimization led to the discovery of a series of 2-anilinothiazole analogs such as 3-(2-((4-hydroxyphenyl)-amino)thiazol-4-yl)phenol **1** (Figure 1) with submicromolar p97 inhibitory potency.¹⁴ However, this series of compounds has also been reported to be active against other enzymes, such as neuropeptide Y5 receptor and sphingosine kinase with a similar potency; therefore, selectivity with this series of

Received: August 31, 2015

Published: November 13, 2015

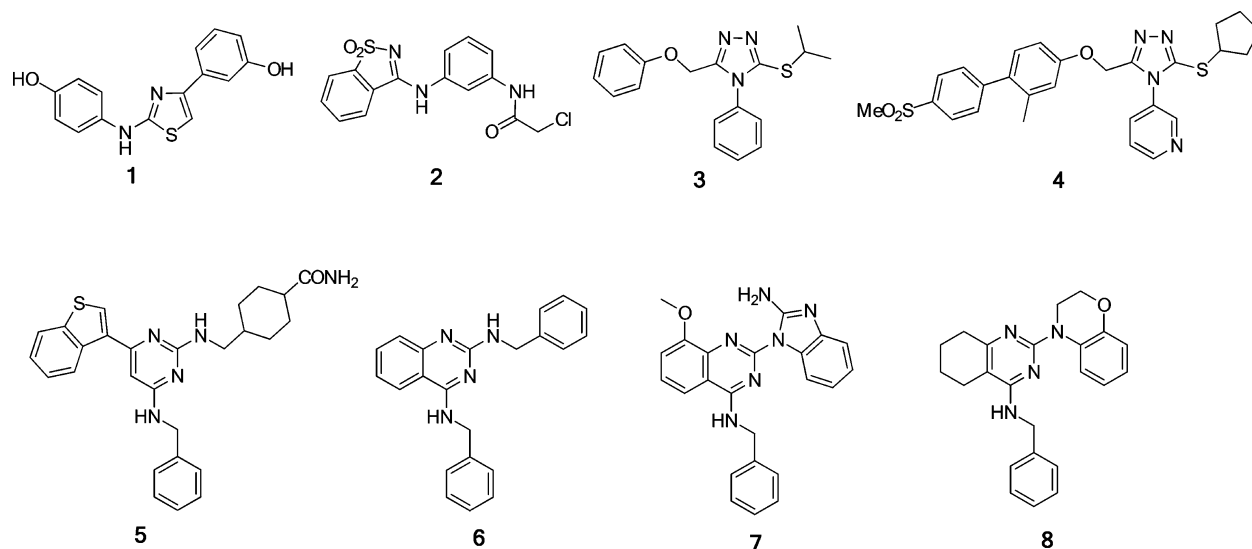


Figure 1. p97 small molecular inhibitors reported in the literature.

compounds could be problematic. 2-Chloro-*N*-(3-((1,1-dioxidobenzo[*d*]isothiazol-3-yl)amino)phenyl)acetamide **2** (NMS-859) was identified from a different HTS campaign as a covalent p97 inhibitor with moderate biochemical and cellular potency (p97i IC_{50} , 0.37 μ M).¹⁵ A more potent allosteric p97 inhibitor came from a series of substituted triazoles, which was discovered by the same group.¹⁶ 3-(Isopropylthio)-5-(phenoxymethyl)-4-phenyl-4*H*-1,2,4-triazole **3** was the initial hit, and structure and activity relationship (SAR) optimization led to its analogue, 3-(3-(cyclopentylthio)-5-(((2-methyl-4'-(methylsulfonyl)-[1,1'-biphenyl]-4-yl)oxy)methyl)-4*H*-1,2,4-triazol-4-yl)pyridine **4** (NMS-873) with the reported IC_{50} of 24 nM against p97 in the biochemical assay and 380 nM of cell killing against HCT 116 cells. However, this compound suffered from extremely poor metabolic stability. A series of cyclohexylamides has also been described.¹⁷ 3-(3-(Cyclopentylthio)-5-(((2-methyl-4'-(methylsulfonyl)-[1,1'-biphenyl]-4-yl)oxy)methyl)-4*H*-1,2,4-triazol-4-yl)pyridine **5** has an IC_{50} of 74 nM in the p97 biochemical assay and an IC_{50} of \sim 5 μ M in an HCT 116 cytotoxicity assay. However, no in vivo antitumor activity has been reported for these molecules.

*N*²,*N*⁴-Dibenzylquinazoline-2,4-diamine **6** (DBeQ) was identified from a HTS as inhibitors of p97 ATPase activity using the NIH compound library.¹⁸ It reversibly inhibits the ATPase function of p97 in an ATP competitive manner. Hit-to-lead optimization efforts resulted in the identification of two analogs, 2-(2-amino-1*H*-benzo[*d*]imidazol-1-yl)-*N*-benzyl-8-methoxyquinazolin-4-amine **7** (ML240) and 2-(2*H*-benzo[*b*]-[1,4]oxazin-4(3*H*)-yl)-*N*-benzyl-5,6,7,8-tetrahydroquinazolin-4-amine **8** (ML241) with almost 10-fold improvement of p97i potency.¹⁹ Compound **7** had good selectivity for inhibition of p97 over a panel of other ATPases and kinases. Recently it has been reported that compounds **7** and **8** preferentially inhibit the D2 ATPase domain of p97.²⁰ While these compounds were valuable research tools, their potency and pharmaceutical properties were insufficient to determine the impact of p97 inhibition in vivo. Herein, we report our lead optimization efforts and SAR analysis leading to the identification of compound **71** (CB-5083), which, to our knowledge, is the first selective p97 inhibitor with the requisite pharmacological properties to allow for testing in clinical trials.

RESULTS

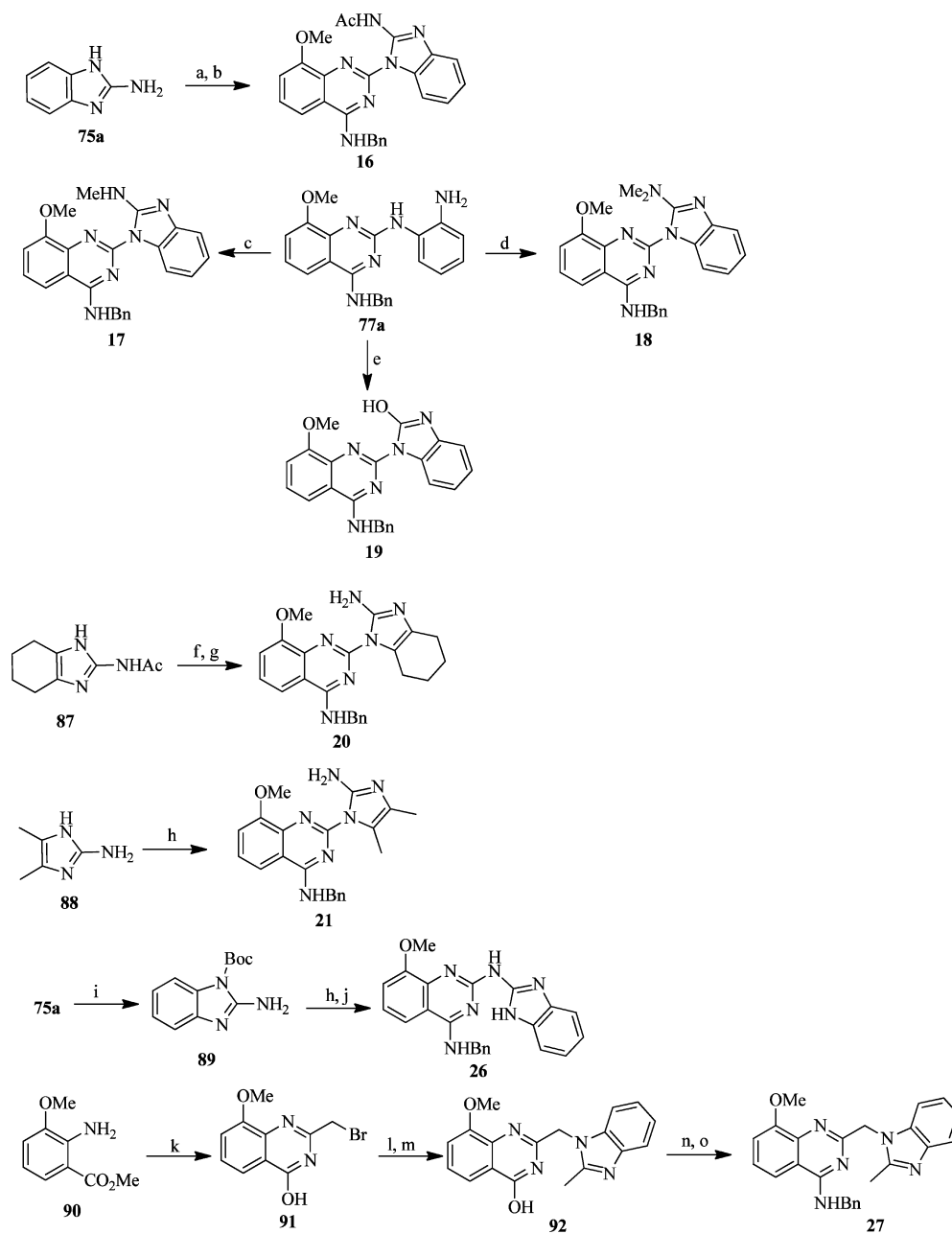
Chemistry. The compound reported to have structure **7** was prepared by coupling of 2-chloroquinazoline **74a** with 2-aminobenzimidazole (**75a**) as shown in Scheme 1.¹⁹ However, it was never unambiguously determined whether the coupling took place on the nitrogen of the imidazole or at the 2-amino group. To verify this, intermediate **74a** was coupled with 1,2-diaminobenzene **76** to yield the intermediate **77a**, which was treated with cyanic bromide to unambiguously form molecule **7**, thus confirming this structural assignment. Analogs (**9**–**11**) were prepared using a similar approach from the corresponding 4-aminoquinazolines **74b**–**d**. 2-Chloro-4-amino-substituted derivative **78**²¹ was acylated with benzoyl chloride to give **79**. By use of a similar two-step procedure as outlined above, analog **12** was obtained in a modest yield. The 4-chloro of **73**, in the presence of a strong base, can be selectively replaced with alcohols such as BnOH to yield intermediate **80**, which was converted into compound **13** through the previously described coupling and cyclization reactions.

Intermediate **73** was reacted with styrylboronic acid **81** in the presence of $Pd(PPh_3)_4$ as a catalyst to regioselectively give 4-styrylquinazoline **82**, which was readily converted into the desired compound **14**. Nitrile **84**²² was reacted with benzylmagnesium bromide followed by cyclization with methyl chloroformate resulting in pyrimidinone **85** which was chlorinated and converted to the corresponding 2-amino-benzimidazole derivative **15** as described previously.

The synthesis of target molecules (**16**–**21**, **26**, **27**) is summarized in Scheme 2. **75a** was acylated²³ and coupled with intermediate **74a** to yield compound **16**. Intermediate **77a** was reacted with isothiocyanatomethane followed by methyl iodide to yield monomethyl compound **17**.²⁴ Treatment of the intermediate **77a** with 2-chloro-1,1,3,3-tetramethylformamidine chloride produced the dimethyl analog **18**.²⁵ **77a** was reacted with carbonyldiimidazole to form the 2-hydroxybenzimidazole derivative **19**. *N*-(4,5,6,7-Tetrahydro-1*H*-benzo[*d*]imidazol-2-yl)acetamide **87**²⁶ was coupled with **74a**, and the acetyl group was removed with hydrazine to form compound **20**. 3,4-Dimethylimidazole **88**²⁷ was reacted with **74a** to give compound **21**. A Boc-protecting group was regioselectively installed onto a nitrogen in the imidazole ring

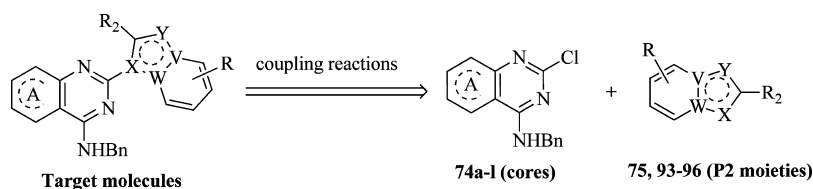
[illegible]

Representative synthetic routes of the (substituted) quinazolines or fused pyrimidines **74e–l** (also referred to as the cores) which possess a chlorine at the 2-position and benzylamino group at the 4-position are illustrated in [Scheme 4](#). Demethylation of 8-methoxyquinazoline **74a** was effected by treatment with boron tribromide. The resulting hydroxyl group on **97** was reacted with 1-bromo-2-methoxyethane to afford the quinazoline **74e**. Dichlorination of the thieno[2,3-*d*]pyrimidin-4-one **98a**^{28,35} followed by condensation with benzylamine gave key intermediate **74f**. In an analogous way, thiazolo[5,4-*d*]pyrimidine diol **98b**²⁹ was used to prepare **74g**. 2-

Scheme 2. Generalized Routes To Synthesize Compounds 16–21, 26, 27^a

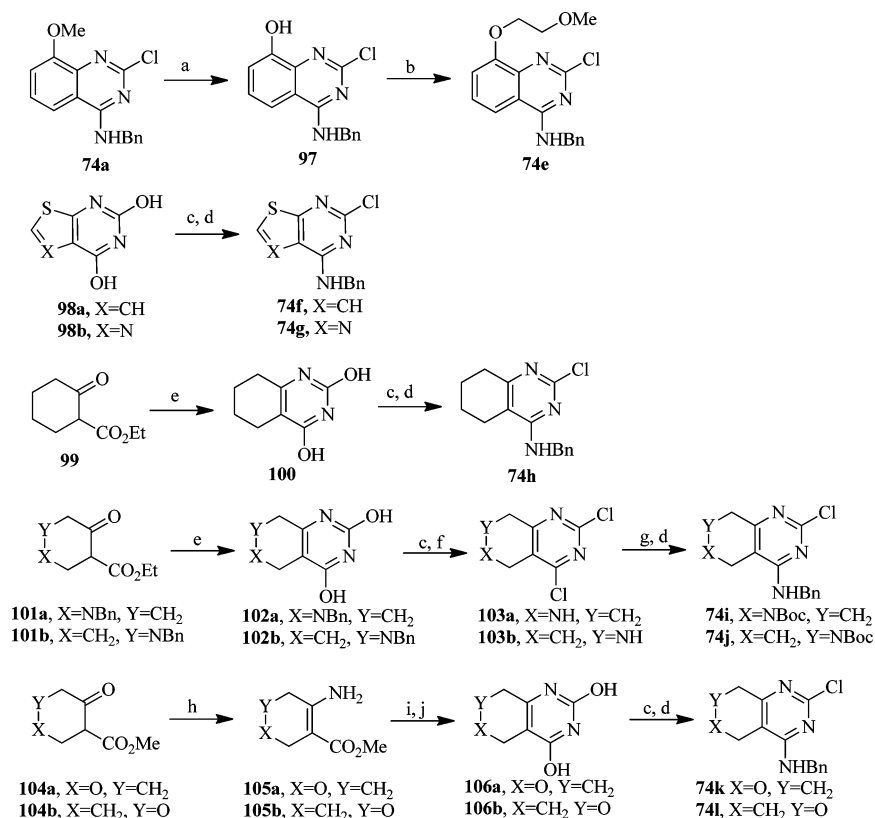
^aReagents and conditions: (a) Ac_2O , TEA, THF, 0 °C; (b) **74a**, $\text{Pd}(\text{dba})_3$, X-Phos, Cs_2CO_3 , dioxane, 100 °C; (c) (1) MeNCS , Et_2O , rt, (2) MeI , EtOH , rt; (d) (1) $\text{Me}_2\text{N}^+=\text{C}(\text{Cl})\text{NMe}_2\cdot\text{Cl}^-$, CHCl_3 , -30 °C, (2) xylene, reflux; (e) CDI , dioxane, 100 °C; (f) **74a**, $\text{Pd}(\text{dba})_3$, *t*-BuPhos, *t*-BuOK, dioxane, 100 °C; (g) NH_2NH_2 , EtOH , H_2O , 70 °C; (h) **74a**, $\text{Pd}(\text{OAc})_2$, BINAP, Cs_2CO_3 , dioxane, 100 °C; (i) $(\text{Boc})_2\text{O}$, TEA, DMF, rt; (j) TFA, DCM, rt; (k) BrCH_2CN , HCl (aq), reflux; (l) **76**, K_2CO_3 , MeCN, 50 °C; (m) $\text{MeC}(\text{OMe})_3$, EtOH , rt; (n) POCl_3 , PhNMe_2 , reflux; (o) BnNH_2 , MeCN, rt.

Scheme 3. Generalized Retrosynthetic Route to the Target Molecules 22–25, 28–38, and 40–72



Oxocyclohexanecarboxylate **99** was easily converted into 2,4-dihydroxypyrimidine **100** which was transformed into the intermediate **74h**. Pyrimidine diols (**102a**, **102b**) were prepared

from ketoesters (**101a**, **101b**)³⁰ and then converted to their corresponding dichlorides using standard methodology. Because of concerns about removal of the benzyl protecting

Scheme 4. Generalized Routes To Synthesize Benzylamino-Substituted Cores 74e–l^a

^aReagents and conditions: (a) BBr₃, DCM, 0 °C; (b) MeO(CH₂)₂Br, DCM, 0 °C; (c) POCl₃, PhNMe₂ or DIPEA, reflux; (d) BnNH₂, MeCN, rt; (e) urea, NaOMe, MeOH, reflux; (f) MeCH(Cl)OCOCl, Cl(CH₂)₂Cl, reflux; (g) Boc₂O, Et₃N, DCM, rt; (h) NH₄OAc, MeOH, rt; (i) Cl₃CCONCO, MeCN, rt; (j) NH₃, MeOH, rt.

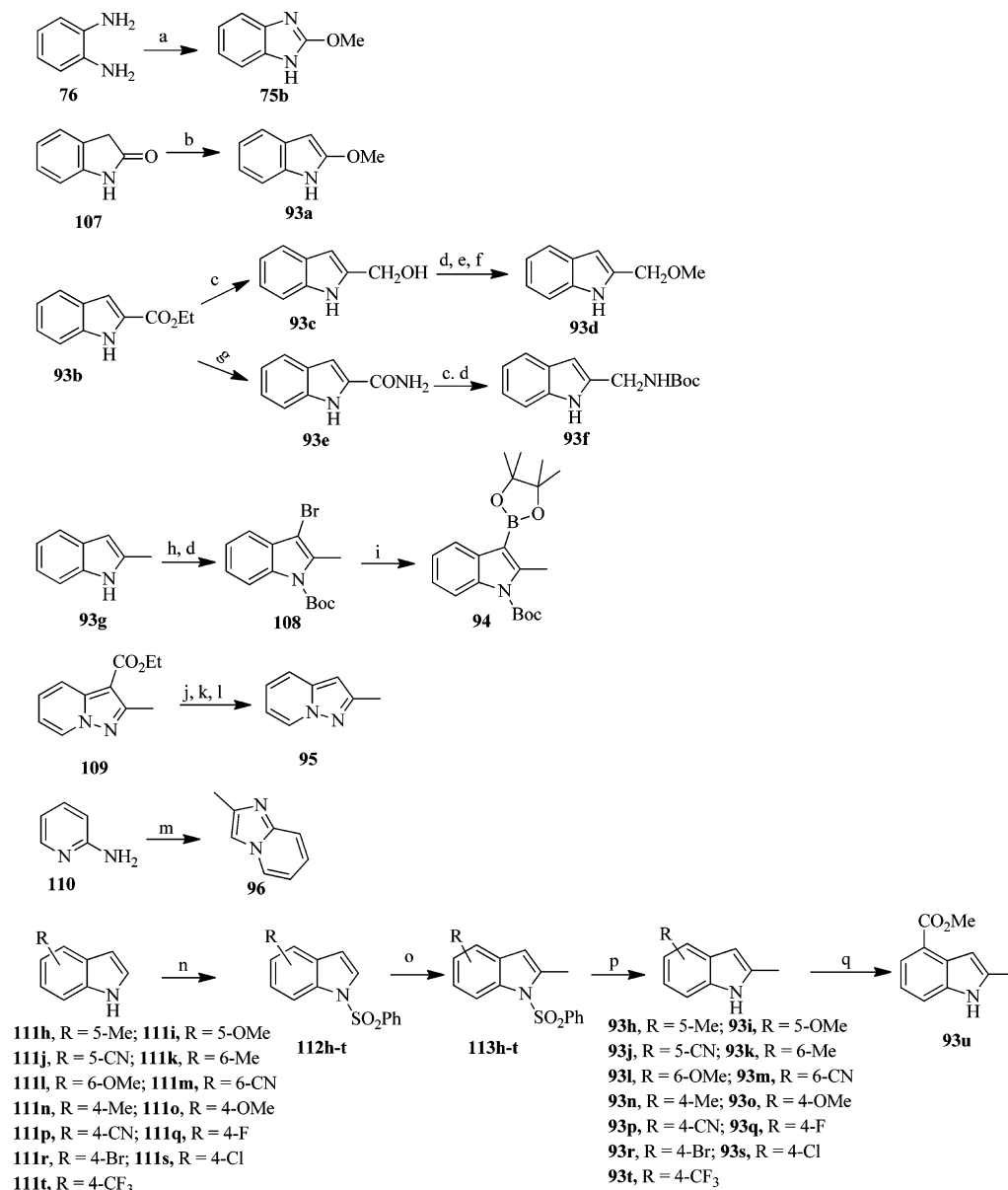
group on the nitrogen of the saturated ring later in the sequence, it was removed at this point using 1-chloroethyl chloroformate giving **103a** and **103b** containing free amine functionality.³¹ The amine functionalities were protected as their *tert*-butyl carbonate derivative, and an *N*-benzyl group was introduced as before to give **74i** and **74j**. Unlike other keto esters, **104a**³² could not withstand the strongly acidic or basic conditions required to catalyze condensation with urea to form a fused pyrimidine. However, it was found that **104a** could be converted to enamine **105a** followed by reaction with 2,2,2-trichloroacetyl isocyanate and cyclization with ammonia to give pyranopyrimidine diol **106a**. Similarly **104b** was converted to pyrimidine diol **106b**. Pyrimidine diols **106a** and **106b** were both converted to their 4-*N*-benzyl-2-chloro derivatives (**74k** and **74l**, respectively) using the previously described conditions.

The 5,6-bicycloheteroaromatic functionalities (also referred to as P2 moieties) that were coupled to the 2-position of the (substituted) quinazolines or fused pyrimidine were either commercially available or were prepared via the approaches summarized in Scheme 5. 2-Methoxy-1*H*-benzo[*d*]imidazole **75b** was prepared by reaction of benzene-1,2-diamine **76** with tetramethyl orthocarbonate under acidic conditions. Methylation of indolin-2-one **107** afforded 2-methoxyindole **93a**. Reduction of ethyl 1*H*-indole-2-carboxylate **93b** using lithium aluminum hydride yielded **93c**, which was methylated to give intermediate **93d**. Reduction of the amide bond of intermediate **93e**, which was prepared from **93b**, followed by Boc-protection gave intermediate **93f**. Bromination followed by *N*-Boc

protection of 2-methylindole **93g** yielded intermediate **108**. Halogen metal exchange with *n*-butyllithium at −78 °C followed by reaction with isopropoxyphenylboronate yielded 3-indolyl boronate **94**. Compound **109**³³ was hydrolyzed, and the resulting acid was converted into the bromide by NBS, and debromination using *n*-butyllithium at a low temperature yielded the desired **95**. 2-Methylimidazo[1,2-*a*]pyridine **96** was prepared in a one-step process wherein 2-aminopyridine **110** was reacted with 1-bromopropan-2-one.

A variety of 4-, 5-, and 6-substituted 2-methylindole derivatives **93h–t** were prepared by a three-step process. Indoles **111h–t** were converted to their corresponding 1-benzenesulfonyl derivatives **112h–t** which were reacted at a low temperature with *n*-butyllithium to effect directed metalation at the 2-position of the indole. Quenching of the resulting anions with methyl iodide produced the 2-methyl derivatives **113h–t**. The benzenesulfonyl group was then removed to give the target indoles. The 2-methyl-1*H*-indole-4-carboxylate derivative **93u** was prepared from 4-bromo-2-methylindole **93r** via a palladium catalyzed carboxylation reaction.

Palladium-catalyzed coupling of the fused pyrimidines **74a–l** with the aforementioned P2 moieties (**75**, **93–96**) yielded the target molecules (**22–25**, **28–38**, and **40–72**) as exemplified in Scheme 6. The substituted quinazolines or fused pyrimidine (**74a**, **74e–i**) were reacted with either the aforementioned benzoimidazoles (**75a**, **75b**) or commercially available benzoimidazole **75c**, 2-methylbenzoimidazole **75d**, 2-ethylbenzoimidazole **75e** in the presence of Pd₂(dba)₃, X-Phos, and cesium carbonate to give target molecules (**22–25** and

Scheme 5. Generalized Routes To Synthesize 5/6 Bicyclic P2 Moieties 75 and 93–96^a

^aReagents and conditions: (a) MeO₄C, AcOH, rt; (b) Me₃OBf₄, CHCl₃, rt; (c) LiAlH₄, THF, 0 °C; (d) (Boc)₂O, DMAP, TEA, DCM, rt; (e) MeI, NaH, THF, 0 °C; (f) TFA, DCM, 0 °C; (g) NH₃, THF, rt; (h) Br₂, DMF; (i) 2-isopropoxy-4,4,5,5-tetramethyl-1,3,2-dioxaborolane, *n*-BuLi, THF, −78 °C; (j) NaOH, MeOH, H₂O, reflux; (k) NBS, NaHCO₃, DMF, 0 °C; (l) *n*-BuLi, THF, −78 °C; (m) MeCOCH₂Br, EtOH, dioxane; (n) PhSO₂Cl, NaH, THF; (o) *n*-BuLi, MeI, THF, −40 °C; (p) NaOH, H₂O, EtOH, 40 °C; (q) Pd(OAc)₂, dppp, TEA, CO, MeOH, reflux.

28–35). In addition to these steps, removal of the Boc protecting group was required for compounds 36–38. Similar coupling reactions between 74h and commercially available indoles such as 2-methylindole 93g, 2-ethylindole 93v, or 2-trifluoromethylindole 93w or the indoles 93a, 93c, 93d, 93f yielded the target molecules 40–46. The 3-indolyl regioisomer 47 was prepared by Suzuki coupling of the fused pyrimidine 74h with boronate 94 followed by deprotection of the indole nitrogen. 2-Methylpyrazolopyridine-containing analogs (48, 49) were made via palladium catalyzed Heck-type coupling between 2-chloropyrimidine 74h and pyrazolopyridines (95, 96), respectively. Similar conditions (Pd₂(dba)₃, X-Phos, and cesium carbonate) were used to carry out Buchwald-type coupling reactions of 74i with the indoles 93g–u to give targets 50–62 and the intermediate 114, respectively. The latter was

hydrolyzed into the acid 63 which was subsequently converted into amides 66–68. Using similar coupling conditions, the 4-carbamoyl-1-indole containing molecules (65, 69–72) were prepared through introduction of the 4-cyano-2-methyl-1-indole (93p) to the 2-position of the fused pyrimidines 74h–l. These intermediates were reacted with palladium acetate and acetaldehyde oxime in the presence of triphenylphosphine to convert the nitrile into the primary carboxamide.³⁴ This methodology was required because coupling with 4-carbamoyl-2-methylindoles either completely failed or resulted in extremely poor yields of the desired products. The intermediate nitrile 115 was reacted with sodium azide followed by acid mediated removal of the *tert*-butylcarbonyl protecting group to provide tetrazine 64.

74a, e-i + **75a, R₂=NH₂**
75b, R₂=OMe
75c, R₂=H
75d, R₂=Me
75e, R₂=Et

22-25, 28-35
X=NBoc
36-38

74h + **93a, R₂=OMe**
93c, R₂=CH₂OH
93d, R₂=CH₂OMe
93f, R₂=CH₂NHBoc
93g, R₂=Me
93v, R₂=Et
93w, R₂=CF₃

40-45
R₂=CH₂NHBoc
46

74h $\xrightarrow{c, d}$ **47**
74h \xrightarrow{e} **95 or 96** \rightarrow **48** or **49**

50-62 $\xleftarrow{a, b}$ **93g-t** \xrightarrow{a} **74i** \xrightarrow{a} **114** $\xrightarrow{f, g, b}$ **66-68**

74h, X=Y=CH₂
74i, X=NBoc, Y=CH₂
74j, X=CH₂, Y=NBoc
74k, X=O, Y=CH₂
74l, X=CH₂, Y=O

93p $\xrightarrow{a, h}$ **69, X=Y=CH₂**
115, X=NBoc, Y=CH₂
65, X=NH, Y=CH₂
116, X=CH₂, Y=NBoc
70, X=CH₂, Y=NH
71, X=O, Y=CH₂
72, X=CH₂, Y=O

64

In Vitro ADME and in Vivo Pharmacokinetics and Pharmacodynamics (PK/PD). Chemical stability was evaluated in simulated gastric and intestinal fluids (SGF and SIF), and the percentage of parent remaining was determined after 15 min incubation. Metabolic stability was assessed in liver microsomes from mouse, rat, dog, monkey, and human; clearance and $T_{1/2}$ were calculated. Permeability was assessed by Caco-2 permeability assays with cultured Caco-2 monolayers; $P_{A \rightarrow B}$ and $P_{B \rightarrow A}$ were determined, and efflux ratio was calculated. Solubility was assessed in a variety of pH buffer solutions. In vivo biological activity was determined in tumor and tissues by PD measurements of the following markers: poly-ubiquitin, CHOP, and cleaved poly ADP-ribose polymerase (cPARP) after oral (po) administration in mice. Absolute

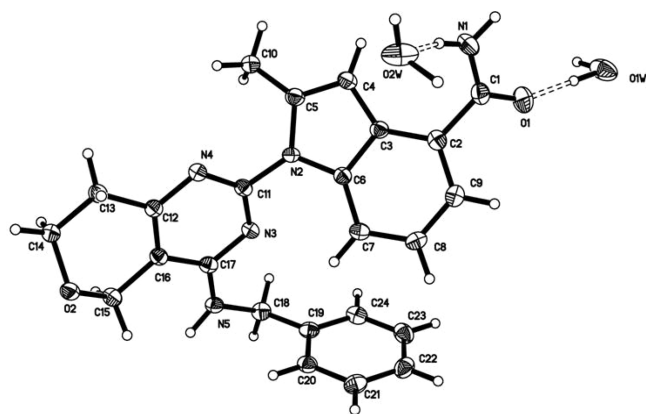


Figure 2. The hydrate contains two molecules of H₂O per molecule of 71.

bioavailability (*F*, %) was determined by the PK assessment of areas under the plasma concentration versus time curves following iv and po administration. Antitumor efficacy was assessed in immunocompromised mice bearing established human tumor xenografts.

DISCUSSION

Initial investigations into the SAR of the 8-methoxyquinazoline series focused on improving potency, selectivity, and pharmaceutical properties so that the postulate of p97 inhibition resulting in antitumor activity in vivo could be tested. During this lead optimization process, we were mindful of the effect that molecular changes could have on physical parameters such as cLogP, LipE, and PSA. The goal was to identify an optimal range of these parameters and consequently to increase potency significantly. The initial strategy involved a systematic evaluation of the functionality of compound 7. We started by investigating the possibility of changing the benzylamino group at the 4-position of the quinazoline. This resulted in compounds that were essentially inactive in the p97 biochemical assay (9–15) as shown in Table 1. Neither simple methylation on methenyl 9 nor nitrogen 10 was tolerated. The benzylamino group could not be replaced by either phenylethylamine 11 or amide 12. Replacement of nitrogen with

either oxygen 13 or carbon 14 as well as deletion of the nitrogen 15 failed to retain the p97 activity. Therefore, the 4-benzylamino group was retained for further optimization. Attention was next focused on the modification of the 2-aminobenzoimidazole moiety found in compound 7 as illustrated in Table 2. Acetylation of the amino functionality at the 2-position of the benzoimidazolyl group resulted in an inactive compound 16. In contrast, either mono or double methylation of the amino group (17 and 18, respectively) increased biochemical potency approximately 4-fold. Replacement of the imidazole ring of benzoimidazole with imidazolone 19 or its phenyl ring by either cyclohexyl 20 or dimethyl 21 failed to increase the p97 potency. The absence of a substituent on the 2-position of benzoimidazolyl 22 lost p97 activity completely. Among the best replacements of the amino group was either methyl 23 or methoxy 25 which led to an approximately 6-fold increase in biochemical potency. Notably, these had only a modest increase in cLogP but did have a significant drop in PSA compared to compound 7. However, larger alkyl groups such as ethyl found in compound 24 were not tolerated. Linking the benzoimidazole and quinazoline functionalities through an amino group on the 2-position of the imidazole or insertion of methenyl as a bridge between them resulted in inactive compounds (26 and 27, respectively).

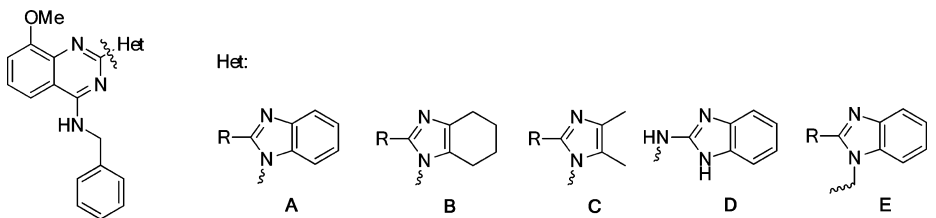
A variety of substituents at the 8-position of the quinazoline and alternatives to the quinazoline core were investigated as exemplified in Table 3. Extensive investigation demonstrated that ether groups were preferred at the 8-position of the quinazoline (data not shown). Solubility was improved by either introducing additional heterofunctionality such as substituted ether groups at the 8-position (28, 29, 30) or replacing the phenyl ring of the quinazoline with five- or six-membered heteroaromatic rings such as thiophene or thiazole (31 and 32, respectively); however, this only resulted in compounds with either similar or only moderately better potency. Efforts to replace the phenyl ring of the quinazoline with saturated five- or six-membered rings led us to identify some more attractive leads that had both enhanced potency and better pharmaceutical properties. The 4,5,6,7-tetrahydroquinazoline core produced compounds that were the most potent p97 inhibitors that we had synthesized to that point (33–35). Compounds 34 and 35 were the first compounds we had seen with an IC₅₀ under 100 nM against p97. Replacement of the quinazoline ring with the 4,5,6,7-tetrahydropyridyl[4,3-*d*]-pyrimidine functionality, which inserted a basic nitrogen into the saturated ring, resulted in compounds with unimpressive p97 biochemical potency (36–38). However, these compounds had markedly lower cLogP and better aqueous solubility, especially in low pH buffer solutions (data not shown).

Compound 35 was notable in that it possessed a 10-fold increase in p97 inhibitory potency compared to the starting point 7. To investigate how 35 interacted with the p97 D1 and D2 ATPase sites, ATP probe 39 (ActivX, San Diego, CA) was utilized to irreversibly label ATP binding sites found in kinases and ATPases. The labeling of ATP sites was measured by mass spectral detection (Figure 3A). Labeling of the proteins existing in the cellular lysates of A549 tumor cells in the presence or absence of 35 was assessed by measuring the abundance of labeled peptide signals after tryptic digest and purification. Compound 35 selectively inhibited labeling at the D2 site of p97 (Figure 3B). This specific interaction with the D2 domain of p97 is consistent with its ability to inhibit the ATPase activity of p97, since the D2 region has been shown to be primarily

Table 1. SAR Expansion on the 4-Position of Quinazoline^a

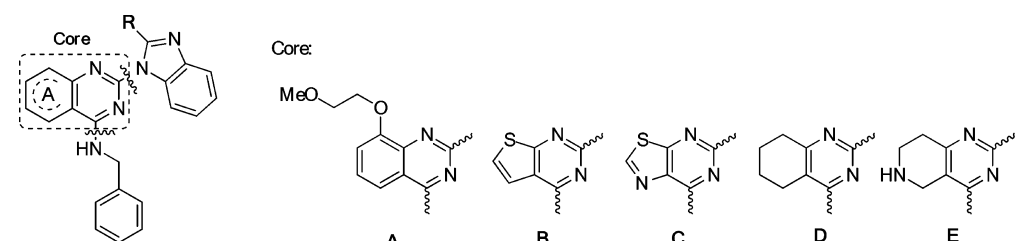
compd	R	p97i IC ₅₀ (μM)	cLogP	PSA
7	NHBn	0.815	4.6	91
9	NHCH(Me)Ph	>5.0	5.0	91
10	N(Me)CH ₂ Ph	>5.0	5.3	82
11	NHCH ₂ CH ₂ Ph	>5.0	4.9	91
12	NHCOPh	>5.0	4.3	108
13	OCH ₂ Ph	>5.0	4.8	88
14	CH ₂ CH ₂ Ph	>5.0	5.0	79
15	CH ₂ Ph	>5.0	4.6	79

^aAll experiments to determine IC₅₀ values were run with at least duplicates at each compound dilution, and all IC₅₀ values were averaged when determined in two or more independent experiments.

Table 2. SAR Expansion on the 2-Position of the Quinazoline^a


compd	Het	R	p97i IC ₅₀ (μM)	cLogP	PSA
16	A	NHAc	>5.0	4.7	94
17	A	NHMe	0.233	5.0	77
18	A	NMe ₂	0.227	5.7	68
19	A	OH	1.068	4.6	79
20	B	NH ₂	>5.0	3.9	91
21	C	NH ₂	>5.0	3.3	91
22	A	H	>5.0	4.5	65
23	A	Me	0.152	4.8	65
24	A	Et	>5.0	5.4	65
25	A	OMe	0.145	5.2	74
26	D		>5.0	5.2	88
27	E	Me	>5.0	5.1	65

^aAll experiments to determine IC₅₀ values were run with at least duplicates at each compound dilution, and all IC₅₀ values were averaged when determined in two or more independent experiments.

Table 3. Assessment of Alternative Fused Pyrimidine Cores^a


compd	core	R	p97i IC ₅₀ (μM)	cLogP	PSA
28	A	NH ₂	0.907	4.4	100
29	A	Me	0.304	4.6	74
30	A	OMe	0.370	5.0	83
31	B	NH ₂	3.000	4.7	82
32	C	OMe	0.180	4.5	78
33	D	NH ₂	0.425	4.6	82
34	D	Me	0.098	4.8	56
35	D	OMe	0.076	5.2	65
36	E	NH ₂	>5.0	3.1	94
37	E	Me	>5.0	3.2	68
38	E	OMe	3.134	3.6	77

^aAll experiments to determine IC₅₀ values were run with at least duplicates at each compound dilution, and all IC₅₀ values were averaged when determined in two or more independent experiments.

responsible for the ATPase activity of p97. In addition, **35** also exhibited in vitro PD effects in A549 tumor cells that are a downstream consequence of specific inhibition of p97 activity (Table 7). These PD effects included dose-dependent accumulation of K48 poly-ubiquitinated proteins as an indication of target engagement and CHOP accumulation and p62 reduction as an indication of pathway inhibition. CHOP is a key transcriptional regulator that is activated through protein accumulation as a result of activation of the UPR.^{37,38} p62 is an adaptor protein that binds to aggregated proteins to target them to the autophagosome.³⁹ When autophagy is activated, p62 protein is degraded as it is

processed through the autophagosome, and therefore measuring p62 protein levels allows for the monitoring of autophagic activity after compound treatment.³⁶ The potency at which these changes occurred was in the same range required to cause A549 cell death. More importantly, **35** demonstrated measurable antitumor activity in mouse xenograft studies when administered orally at the dose of 300 mg/kg on a daily basis (see Supporting Information S1). Taken together, these data indicated that potent and specific binding to the D2 ATPase domain could lead to p97 ATPase inhibition which in turn could induce tumor cell death both in vitro and in vivo by interfering with this vital protein homeostasis pathway.

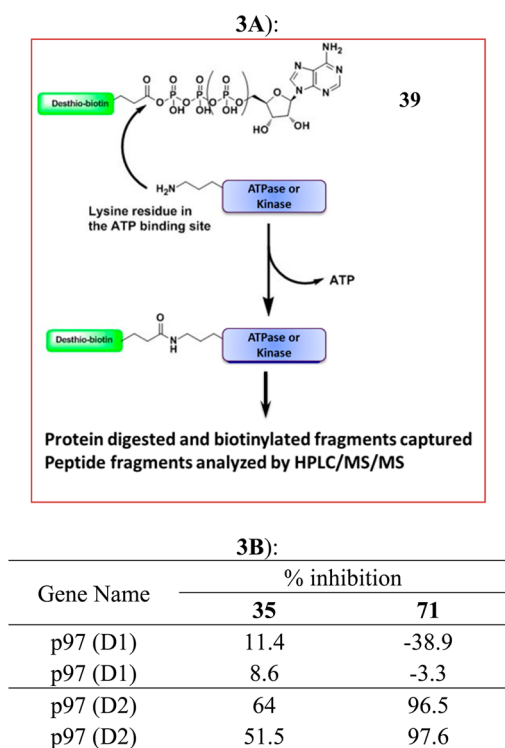


Figure 3. Compounds **35** and **71** selectively inhibit p97 through its D2 site. (A) Illustration of ActivX's competitive ATPase assay. (b) Percentage of inhibition was determined by treatment with 10 μ M compounds **35** and **71**.

While compound **35** provided important proof of concept, further improvement of potency and metabolic stability was still required to achieve a viable drug candidate. Therefore, further optimization of the potency and pharmaceutical properties of this series of p97 inhibitors was undertaken. Since analogs with either methyl or methoxy group at the 2-position of benzimidazole consistently showed more potent p97 activity, we decided to investigate whether benzimidazole itself could

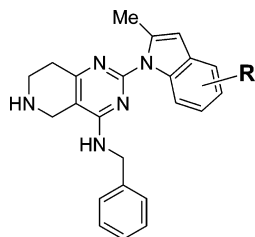
be further optimized by replacement with other 5,6-bicycloaromatic rings with either methyl or methoxy on the 2-position using 4,5,6,7-tetrahydroquinazoline as the core (Table 4). Indeed, the benzimidazole was found to be replaceable. Both compounds (**40**, **41**) containing 1-indolyl functionality on their 2-position were approximately 3-fold more potent, with IC_{50} values under 50 nM, compared to their benzimidazole analogs (**13**, **15**, respectively). As in the benzimidazole subseries, at the 2-position of the indole, the bigger alkyl groups such as ethyl **42** or electron withdrawing moieties such as trifluoromethyl **43** caused a loss of potency. However, the hydroxymethyl analog **44** retained a similar potency in terms of p97 inhibition and cell killing, though its methyl ether derivative **45** had dramatically reduced potency most likely due to the limited tolerability of the size of the substituent at the 2-position of indole. We next turned our efforts to introducing basic moieties with the aim of increasing solubility. An aminomethyl in compound **46** is tolerated with slightly weaker potency but retained its capacity for killing cells. It was also found that 3-indole **47** or regional isomers of 1-benzimidazole, 3-(2-methylpyrazolo[1,5-*a*]pyridinyl) **48**, and 3-(2-methylimidazo[1,2-*a*]pyridinyl) **49** were all tolerated with slightly less activity. Compound **50** had lower biochemical potency but had excellent solubility and liver microsomal stability (Table 7). The introduction of the basic amino group caused a significant decrease in cLogP, and despite its decreased potency, it had one of the largest LipE values observed to that point. In addition, it was noticed that most of these compounds still possessed relatively low PSA.

In an effort to improve the potency of compound **50**, the substitution pattern on the phenyl ring of the indole moiety was systematically investigated (Table 5). Initially, we intended to introduce neutral, electron donating, or electron withdrawing substituents (methyl, methoxy, and cyano, respectively) into all positions of its phenyl ring (4-, 5-, 6-, and 7-position). However, it turned out to be a challenge to couple 7-substituted 1-indoles with the 2-chloro-substituted core, most likely due to steric factors, and therefore only nine derivatives

Table 4. Investigation of Alternative 2-Position Heterocycles^a

			Het:					
				A	B	C	D	
compd	X	Het	R	p97i IC_{50} (μ M)	A549 CTG IC_{50} (μ M)	cLogP	PSA	
40	CH ₂	A	Me	0.047	6.53	5.4	43	
41	CH ₂	A	OMe	0.043	7.11	5.1	52	
42	CH ₂	A	Et	0.445	ND	5.9	43	
43	CH ₂	A	CF ₃	0.651	>40	6.1	43	
44	CH ₂	A	CH ₂ OH	0.068	8.4	4.3	63	
45	CH ₂	A	CH ₂ OMe	0.795	>40.0	4.9	52	
46	CH ₂	A	CH ₂ NH ₂	0.153	4.7	4.3	69	
47	CH ₂	B	Me	0.149	15.84	5.9	54	
48	CH ₂	C	Me	0.367	25	5.5	55	
49	CH ₂	D	Me	0.248	18.21	4.7	55	
50	NH	A	Me	0.192	8.64	3.9	55	

^aAll experiments to determine IC_{50} values were run with at least duplicates at each compound dilution, and all IC_{50} values were averaged when determined in two or more independent experiments.

Table 5. Substitution on Phenyl Ring of the Indole^a

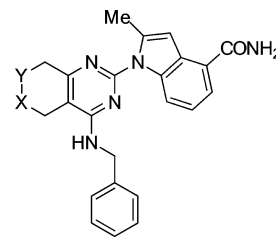
compd	R	p97i IC ₅₀ (μM)	A549 CTG IC ₅₀ (μM)	cLogP	PSA
51	5-Me	>5.0	ND	4.3	55
52	5-OMe	>5.0	ND	3.6	64
53	5-CN	>5.0	ND	3.7	79
54	6-Me	3.860	ND	4.3	55
55	6-OMe	>5.0	ND	3.6	64
56	6-CN	8.908	ND	3.7	79
57	4-Me	0.648	7.85	4.3	55
58	4-OMe	2.075	ND	3.6	64
59	4-CN	0.144	8.92	3.7	79
60	4-F	0.342	6.28	4.0	55
61	4-Cl	0.632	7.24	4.4	55
62	4-CF ₃	3.912	ND	4.7	55
63	4-CO ₂ H	0.095	>40.0	0.4	92
64	4-(5-tetrazolyl)	0.015	>40.0	1.2	109
65	4-CONH ₂	0.040	2.33	2.5	98
66	4-CONHMe	0.215	6.03	2.8	84
67	4-CONMe ₂	>5.0	ND	3.0	75
68	4-CONHCHMe ₂	4.832	ND	3.5	84

^aAll experiments to determine IC₅₀ values were run with at least duplicates at each compound dilution, and all IC₅₀ values were averaged when determined in two or more independent experiments.

(51–59) were prepared successfully. It was found that substitution on either 5- or 6-position of the indole nucleus resulted in complete or substantial losses in p97 potency. While substitution was generally better tolerated at the 4-position of the indole, only the 4-cyano substituted indole **59** showed somewhat greater potency. Therefore, a variety of other electron withdrawing moieties (**60–68**) were introduced into this position. The primary amide **65** turned out to be the best in terms of biochemical and cell killing potency. The acid **63** and tetrazole derivatives **64** were biochemically potent but inactive in cell killing, most likely owing to their zwitterionic nature. Consistent with the observation, the PSA of these more potent compounds increased to a range of 70–100.

With this finding, we decided to keep the moiety of 1-(2-methyl-4-carbamoylindolyl) as the substituent on the 2-position and the *N*-benzylamino moiety at the 4-position of the pyrimidine and then screened a number of fused pyrimidine cores, representatives of which are summarized in Table 6. All of these compounds demonstrated good p97 potency. Among them, 5,6,7,8-tetrahydroquinazoline **69** and 7,8-dihydro-5H-pyrano[4,3-*d*]pyrimidine **71** were the most potent in terms of both p97 enzyme inhibition (IC₅₀ < 15 nM) and tumor cell killing (submicromolar IC₅₀). They also caused significant K48 poly-ubiquitinated protein and CHOP accumulation as well as p62 reduction at submicromolar concentrations after a 6 h treatment as a consequence of p97 inhibition in cells (Table 7). They also possessed reasonable cLogP and PSA.

LipE is an easily calculated metric that assesses the contribution of nonspecific hydrophobic interactions to

Table 6. Exploration of Fused Ring Substituents^a

compd	X	Y	p97i IC ₅₀ (μM)	A549 CTG IC ₅₀ (μM)	cLogP	PSA
69	CH ₂	CH ₂	0.006	0.59	4.1	86
70	CH ₂	NH	0.071	2.44	2.6	98
71	O	CH ₂	0.011	0.68	2.7	95
72	CH ₂	O	0.023	1.07	2.8	95

^aAll experiments to determine IC₅₀ values were run with at least duplicates at each compound dilution, and all IC₅₀ values were averaged when determined in two or more independent experiments.

potency, and representative molecules' LipEs are shown in Table 7.⁴⁰ Use of this metric assumes that compounds whose biochemical potency is driven by a specific interaction with the biological target to a degree greater than would be expected by a simple increase in lipophilicity will tend to be more "druglike".⁴¹ An analysis of LipE of key compounds in this SAR study showed a continual increase in this parameter from the initial starting point of compound **7** (LipE = 1.50) to compound **35** (LipE = 1.95) and compound **50** (LipE = 2.87) which had improved potency with similar or somewhat lower cLogP values. The introduction of the amide onto the 4-position of the indole produced a series of compounds with consistently higher LipE values. Compound **65** had a significantly improved LipE and the best overall cellular potency within its subseries (see Table 7), while compound **69** possessed a slightly lower overall LipE but higher cellular potency. Compound **71** had the highest LipE value (LipE = 5.20) and excellent cellular potency.

The two most in vitro potent molecules (**69**, **71**) were then profiled in vivo using tumor-bearing mice to evaluate their PK and PD effect and antitumor activity. Both molecules were administered orally as a suspension in 0.5% methylcellulose aqueous suspensions at the fixed dose strength of 150 mg/kg; plasma and tumor samples at multiple time points (2, 6, 16, and 24 h) were harvested for PK/PD analysis (Figure 4). **71** had an approximately 2-fold higher exposure in both plasma and tumor compared to **69**. **71** also achieved a more sustained PD effect of poly-ubiquitinated protein accumulation in tumor, especially at later time points. Antitumor activity of the two compounds was assessed in an HCT 116 tumor xenograft model. **71** was administered orally using every day (qd) dosing, whereas **69** was administered every other day (q2d). **71** showed more profound antitumor activity in this study (Figure 5). In addition, **71** has a better aqueous solubility than **69** (Table 7) and has good metabolic stability with a 102 min *T*_{1/2} in a mouse liver microsomal stability study and a 172 min *T*_{1/2} in a hepatocyte stability study. It also has excellent permeability as assessed in a Caco-2 assay (Table 8). PK studies revealed that **71** has moderate absolute oral bioavailability (41%) in mouse (Table 9), making it suitable for preclinical development. Therefore, **71** was selected for further in vitro and in vivo evaluation.

Table 7. Comparison of Calculated Physicochemical Properties Values of Key Compounds for Developing SAR^a

compd	IC ₅₀ (μM)					MLM T _{1/2} (min)	aqueous solubility (mg/mL)	LipE
	p97i	A549 CTG	A549 K48	A549 CHOP	A549 p62			
7	0.815	3.26	6.14	6.61	NA	7	<0.001	1.46
35	0.076	7.45	4.24	9.34	4.84	11	<0.001	1.95
50	0.192	8.64	15.32	9.15	NA	stable	0.75	2.87
65	0.04	2.33	1.79	2.86	2.00	105	1.255	4.89
69	0.006	0.59	0.50	0.58	0.25	44	0.004	4.14
71	0.011	0.68	0.68	1.03	0.49	102	0.032	5.2

^aAll experiments to determine IC₅₀ values were run with at least duplicates at each compound dilution, and all IC₅₀ values were averaged when determined in two or more independent experiments.

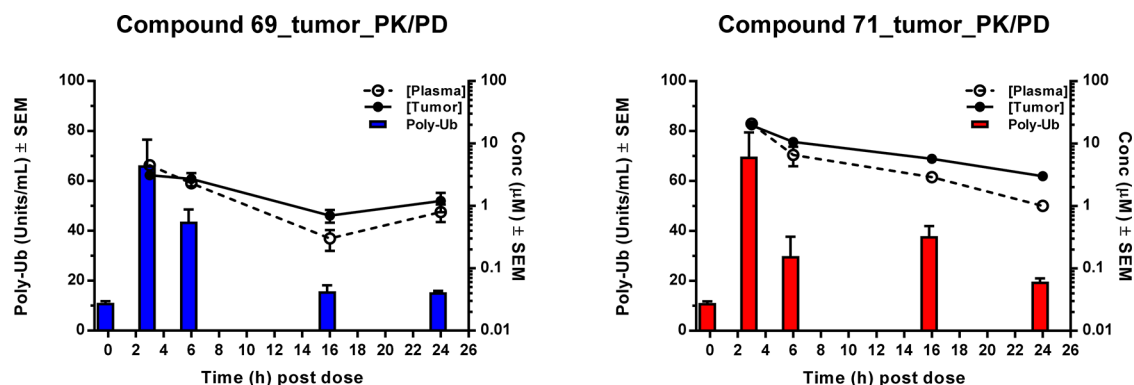


Figure 4. Mouse PK exposure and PD poly-ubiquitinated proteins accumulation for measurement of target engagement. Nu/Nu nude female mice bearing established human A549 lung carcinoma were treated by a single dose of compounds **69** and **71** via oral administration at a dose of 150 mg/kg each, formulated as suspension in 0.5% methylcellulose in water. Animals were harvested at the aforementioned time points, and plasma and tumor tissue samples were collected for PK/PD analysis.

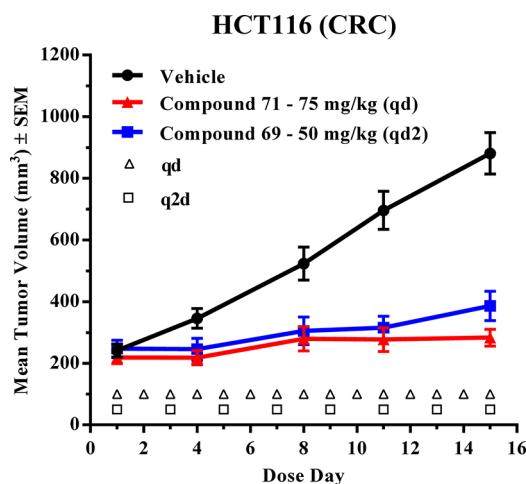


Figure 5. Antitumor response induced by oral administration of compounds **69** and **71**. Nu/Nu nude female mice bearing established human tumor xenografts derived from HCT 116 colon were treated for 2 weeks. Compounds were formulated as suspension in 0.5% methylcellulose in water. *N* = (8–10)/group. Dose: compound **69** (50 mg/kg, qd2) and **71** (75 mg/kg, qd).

The specificity of the interaction of **71** with p97 was assessed in multiple ways. In A549 cellular lysates, **71** selectively blocks the interaction of the irreversible ATP probe **39** with the D2 region of p97 at 10 μM concentration to a greater extent than was observed with **35** with no interaction with the p97 D1 site (Figure 3B). It showed little or no interaction with a panel of over 300 other ATPases, helicases, and kinases that were also assessed in this assay (Table 8).³⁶ A modest interaction was

observed with the kinase DNAPK. The biochemical IC₅₀ of **71** was determined to be >60-fold weaker for DNAPK compared to p97, and no evidence of cellular effects of inhibition of this kinase has been observed.³⁶

Cell lines that were resistant to **71** were generated and were found to contain specific mutations in the p97 D2 ATPase region, N660 and T688 (data not shown). **71** had a ~50-fold reduction in potency when tested on recombinant p97 carrying these mutations.³⁶ Combining this information with the aforementioned SAR analysis allowed us to investigate possible binding modes of **71** with p97. **71** was docked into the D2 ATP binding site. AutoDock Vina is the software used to execute docking of the compound into the active site of p97. The search was performed within a box of 30 × 30 × 30 Å³ centered at the ATP binding site. The side chains of a set of protein residues lining the ATP binding pocket were allowed to adjust during the docking procedure. The top 15 poses ranked by binding energy were examined visually, and the best pose consistent with the SAR and mutation data was selected for further analysis. The obtained docking pose (Figure 6) shows that not only multiple hydrogen bonds are potentially formed between the 2-nitrogen of the pyrimidine core and the NH of the benzylamino group with the aforementioned two amino acids but also the benzyl group fits into a tight hydrophobic pocket, which is consistent with our SAR and the reported 5 binding model.¹⁷ The profound potency improvement of the primary amide on the 4-position of the indole, compared to its cyano-substituted or nonsubstituted analogs, may suggest that the capacity of this amide as both a hydrogen bond donor and acceptor is critical. Indeed, according to this model, this amide may interact with both amino acids S664 and K663. Therefore,

Table 8. In Vitro Potency, Selectivity, and in Vitro ADME Profile of Compound 71

assay	result
p97 biochemical IC ₅₀	11 nM
cell based IC ₅₀ for cell killing	115–2000 nM (>300 tumor cell lines tested)
cell based IC ₅₀ for poly-Ub accumulation	150–800 nM (12 tumor cell lines tested)
off target ATPase inhibition	0/175
off target kinase inhibition	1/173; DNAPK (IC ₅₀ = 500 nM; inactive in cells)
mouse liver microsomal stability (<i>T</i> _{1/2})	102 min
mouse hepatocytes stability (<i>T</i> _{1/2})	172 min
Caco-2 permeability {[<i>P</i> _{app} , A–B (10 ^{−6} cm/s)]/efflux}	52.4/0.7

Table 9. Single-Dose Plasma Pharmacokinetics of Compound 71 in Female Nude Mice^a

iv Administration							
dose (mg/kg)	$t_{1/2}$ (h)	C_0 (μ M)	AUC_{last} (h $\cdot\mu$ M)	AUC_{Inf} (h $\cdot\mu$ M)	V_{ss} (mL/kg)	CL (mL min ⁻¹ kg ⁻¹)	MRT (h)
3.0	2.83	25.7	8.38	8.42	418.0	5.9	1.17
po Administration							
dose (mg/kg)	$t_{1/2}$ (h)	t_{max} (h)	C_{max} (μ M)	AUC_{last} (h $\cdot\mu$ M)	AUC_{Inf} (h $\cdot\mu$ M)	MRT (h)	F (%)
25	2.56	0.50	7.95	28.89	28.94	3.05	41

^aiv formulation vehicle: solution in PEG300/TPGS/EtOH/water (40:10:5:45, v/v/v/v). po dose formulation vehicle: suspension in 0.5% (v/v) MC in water (v/v). *n* = 4 animals per study.

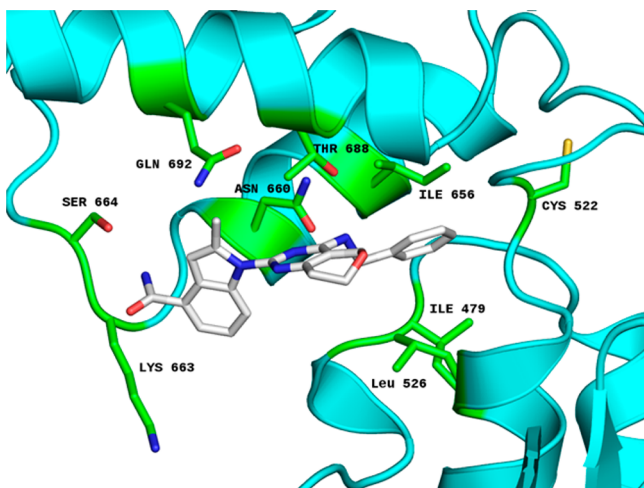


Figure 6. Proposed compound 71 dock model at p97 D2 binding site.

71 may compete with ATP for the same binding site but perhaps through a slightly different orientation.

The oral antitumor activity of 71 was compared to the proteasome inhibitor, bortezomib, in both a multiple myeloma model (AMO-1) and a solid tumor model (A549 lung carcinoma) as summarized in Figure 7. Bortezomib was administered at its reported efficacious dose strength, administration route (iv), and schedule. 71 was administered orally at a dose of 100 mg/kg as a suspension in 0.5% methylcellulose aqueous solution on a (qd4 on)/(−3 off) weekly schedule. Both compounds were active in the AMO-1 multiple myeloma model. However, only 71 was active in the A549 lung carcinoma model, and bortezomib was inactive. This provides preclinical evidence that p97 inhibitors can potentially be effective against both hematologic and solid tumors.

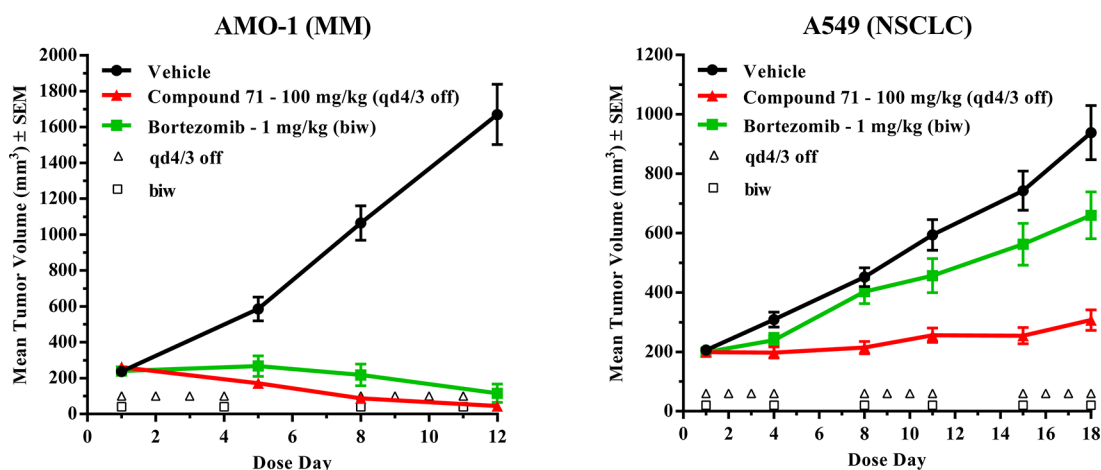


Figure 7. Antitumor response induced by oral administration of compound 71. Nu/Nu SCID beige female mice bearing established human tumor xenografts derived from AMO-1 multiple myeloma and A549 lung carcinoma were treated for up to 3 weeks. *N* = (8–10)/group. Dose: compound 71 (60 or 100 mg/kg, (qd4 on)/(−3 off)) as a suspension in 0.5% methylcellulose in water. Control (bortezomib) was dosed at its reported efficacy doses, schedule, and administration route.

CONCLUSIONS

Through a systematic SAR optimization, we have discovered **71**, a potent and selective inhibitor of the p97 D2 site with nanomolar biochemical and submicromolar cellular potency and moderate oral bioavailability. In vivo **71** caused rapid and sustained accumulation of poly-ubiquitinated proteins and markers of the UPR and apoptosis as well as demonstrated significant tumor growth inhibition in solid tumor and hematological xenograft models. **71** (CB-5083) was nominated as a drug candidate for the treatment of cancer and is currently being tested in ongoing phase 1 clinical trials for patients with relapsed/refractory multiple myeloma and advanced solid tumors.

EXPERIMENTAL SECTION

General Methods. Chemicals, reagents, and solvents were obtained from commercial sources, and they were used as received. NMR spectra were obtained in CDCl₃, DMSO-*d*₆, CD₃OD, or acetone-*d*₆ at 25 °C at 300 MHz on an OXFORD (Varian) with chemical shift (δ , ppm) reported relative to TMS as an internal standard. HPLC–MS chromatograms and spectra were obtained with Shimadzu LC-MS-2020 system, and UV absorption was recorded at wavelengths of 214 and 254 nm using acetonitrile and water under either acidic conditions (i.e., 0.1% HCO₂H, HCl, or TFA) or neutral conditions (i.e., 0.1% NH₄OAc) as the mobile phases. Preparative reverse phase HPLC instruments were Gilson GX-281 (Gilson) and P230 Preparative Gradient System (Elite) using the aforementioned mobile phases. Microwave instrument was CEM Discover SP. Normal phase flash chromatography was performed on silica gel 60. All final compounds were purified to >95% purity as determined by HPLC and ¹H NMR spectra.

Chemistry. N-Benzyl-2-chloro-5,6,7,8-tetrahydroquinazolin-4-amine (74h). *Step 1: 5,6,7,8-Tetrahydroquinazoline-2,4-diol (100).* To a room temperature HCl solution in ethanol (3 N, 250 mL) were added urea (26.5 g, 441 mmol) and 2-oxocyclohexanecarboxylate (**99**) (50.0 g, 294 mmol), and the resulting solution was refluxed overnight. It was then cooled to room temperature and the precipitated white solids were collected to yield the diol (**100**) (14.0 g, 28.6%) which was used in the next step without further purification. LRMS (M + H⁺) *m/z*: calcd 167.1; found 167.1.

Step 2: 2,4-Dichloro-5,6,7,8-tetrahydroquinazoline. A mixture of the crude diol (**100**) (14 g, 84.3 mmol) in POCl₃ (100 mL) was refluxed for 2 h. After being cooled to room temperature, the mixture was concentrated in vacuo. DCM (200 mL) and ice–water (100 mL) were added, the separated organic layer was dried over sodium sulfate and concentrated in vacuo, and the residue was purified by flash chromatography (silica gel, petroleum ether, ethyl acetate) to afford the dichloride 5,6,7,8-tetrahydroquinazoline (16.3 g, 95%). ¹H NMR (300 MHz, CDCl₃): δ 2.85–2.82 (m, 2H, CH₂), 2.56–2.53 (m, 2H, CH₂CN), 1.84–1.78 (m, 4H, (CH₂)₂).

Step 3: N-Benzyl-2-chloro-5,6,7,8-tetrahydroquinazolin-4-amine (74h). To a room temperature solution of the aforementioned crude dichloride (16 g, 79 mmol) in acetonitrile (200 mL) was added phenylmethanamine (25 g, 240 mmol), and the reaction mixture was stirred at the same temperature overnight. The solvents were then removed in vacuo, and the residue was dissolved with dichloromethane (200 mL) and washed with saturated ammonium chloride solution. The separated organic layer was concentrated and the residue was purified by column chromatography (silica gel, petroleum ether, ethyl acetate) to give the key intermediate (**74h**) (20 g, 93%). ¹H NMR (300 MHz, CDCl₃): δ 7.33–7.20 (m, 5H, Ph), 4.64 (s, 2H, CH₂Ph), 2.58 (t, *J* = 5.1 Hz, 3H, CH₂), 2.35 (t, *J* = 5.1 Hz, 2H, CH₂), 1.84–1.78 (m, 4H, (CH₂)₂).

N-tert-Butyl 4-(benzylamino)-2-chloro-7,8-dihydropyrido[4,3-d]pyrimidine-6(5H)-carboxylate (74i). *Step 1: 6-Benzyl-5,6,7,8-tetrahydropyrido[4,3-d]pyrimidine-2,4-diol (102a).* To a room temperature solution of ethyl 1-benzyl-4-oxopiperidine-3-carboxylate (**101a**) (50 g, 0.19 mol) in methanol (100 mL) were

added urea (23 g, 0.38 mol) and sodium methoxide (21 g, 0.38 mol), and then the reaction mixture was refluxed for 48 h. It was then cooled to room temperature, and the precipitated solids were collected, washed with water (50 mL \times 3), and dried to yield the diol (**102a**) (32 g, 65%). LRMS (M + H⁺) *m/z*: calcd 258.1; found 258.1. ¹H NMR (300 MHz, DMSO-*d*₆): δ 7.32–7.23 (m, 5H, Ph), 3.57 (s, 2H, CH₂Ph), 2.97 (s, 2H, NCH₂), 2.56 (t, *J* = 6 Hz, 2H, NCH₂CH₂), 2.29 (t, *J* = 6 Hz, 2H, NCH₂CH₂).

Step 2: 6-Benzyl-2,4-dichloro-5,6,7,8-tetrahydropyrido[4,3-d]pyrimidine. A solution of the aforementioned diol (**102a**) (15 g, 0.058 mol) in POCl₃ (200 mL) was refluxed and stirred for 3 h. After being cooled to room temperature, the mixture was concentrated in vacuo. The residue was diluted with dichloromethane (200 mL) and water (100 mL) and neutralized with sodium hydroxide. The aqueous phase was separated and extracted with dichloromethane (50 mL \times 2). The combined organic layers were washed with brine, dried over anhydrous sodium sulfate, and concentrated in vacuo. The residue was dried to give 6-benzyl-2,4-dichloro-5,6,7,8-tetrahydropyrido[4,3-d]pyrimidine (13.5 g, yield = 79%, purity > 95%), which was used in the next step without further purification. LRMS (M + H⁺) *m/z*: calcd 294.05; found 294.1.

Step 3: 2,4-Dichloro-5,6,7,8-tetrahydropyrido[4,3-d]pyrimidine (103a). To a room temperature solution of the aforementioned crude dichloride (13.5 g, 46 mmol) in 1,2-dichloroethane (120 mL) was added 1-chloroethyl carbonochloridate (19.7 g, 138 mmol). Then the solution was refluxed for 3 h. The solution was cooled and concentrated in vacuo. The residue was dissolved in methanol (120 mL) and refluxed for another 30 min. It was cooled and concentrated in vacuo to give the crude 2,4-dichloro-5,6,7,8-tetrahydropyrido[4,3-d]pyrimidine (**103a**) (9.0 g, 97%), which was used in the next step without further purification. LRMS (M + H⁺) *m/z*: calcd 204.0; found 204.0.

Step 4: N-tert-Butyl-2,4-dichloro-5,6,7,8-tetrahydropyrido[4,3-d]pyrimidine. To a room temperature solution of the aforementioned crude intermediate (**103a**) (9.0 g, 44.3 mmol) in dichloromethane (90 mL) were added (Boc)₂O (11.5 g, 53 mmol) and Et₃N (18.5 mL, 133 mmol). Then the mixture was stirred at the same temperature for 2 h. The reaction solution was washed with water (100 mL \times 2) and brine (50 mL); the separated organic layer was concentrated in vacuo to give the crude *N-tert-butyl* 2,4-dichloro-5,6,7,8-tetrahydropyrido[4,3-d]pyrimidine (13.0 g, yield = 97%, purity = 95%), which was used in the next step without further purification. LRMS (M + H⁺) *m/z*: calcd 304.1; found 303.9.

Step 5: N-tert-Butyl 4-(benzylamino)-2-chloro-7,8-dihydropyrido[4,3-d]pyrimidine-6(5H)-carboxylate (74i). To a room temperature solution of the aforementioned crude Boc-protected 2,4-dichloride (13.0 g, 43 mmol) in acetonitrile (90 mL) were added phenylmethanamine (7.0 g, 65 mmol) and triethylamine (18 mL, 129 mmol). The resulting solution was then stirred at the same temperature overnight and concentrated in vacuo; the residue was purified by flash chromatography (silica gel, petroleum ether, ethyl acetate) to afford *N-tert-butyl* 4-(benzylamino)-2-chloro-7,8-dihydropyrido[4,3-d]pyrimidine-6(5H)-carboxylate (**74i**) (13.0 g, yield = 81%). LRMS (M + H⁺) *m/z*: calcd 375.2; found 375.1. ¹H NMR (300 MHz, CDCl₃): δ 7.36–7.34 (m, 5H, Ph), 4.84 (br, 1H, NH), 4.70 (s, 2H, CH₂Ph), 4.19 (s, 2H, NCH₂), 3.68 (t, *J* = 5.7 Hz, 2H, NCH₂CH₂), 2.79 (t, *J* = 5.7 Hz, 2H, NCH₂CH₂), 1.49 (s, 9H, C(CH₃)₃).

N-Benzyl-2-chloro-7,8-dihydro-5H-pyrano[4,3-d]pyrimidin-4-amine (74k). *Step 1: 7, 8-Dihydro-5H-pyrano[4,3-d]pyrimidine-2,4-diol (106a).* Methyl 4-oxotetrahydro-2H-pyran-3-carboxylate (**104a**) (1.58 g, 10 mmol) and ammonium acetate (2.3 g, 30 mmol) in methanol (20 mL) were stirred at room temperature overnight. The mixture was concentrated in vacuo, dichloromethane (100 mL) and water (20 mL) were added, and the separated organic layer was dried over sodium sulfate and concentrated in vacuo. The resulting crude methyl 4-amino-5,6-dihydro-2H-pyran-3-carboxylate (**105a**) was then dissolved in acetonitrile (20 mL), and 2,2,2-trichloroacetyl isocyanate (3.76 g, 20 mmol) was added. The resulting mixture was stirred for 30 min, and the precipitated solids were collected and dissolved in a solution of ammonia in methanol (8 mL, 7 N). Then the resulting

mixture was heated at 70 °C for 2 h. The reaction was cooled down and the precipitated solids were collected and dried to afford the diol (**106a**) (1.2 g, 71%, purity ≈ 99%). LRMS ($M + H^+$) m/z : calcd 169.1; found 169.0. 1H NMR (300 MHz, DMSO- d_6): δ 10.98 (br, 2H, 2OH), 4.19 (s, 2H, OCH₂), 3.76 (t, J = 5.4 Hz, 2H, OCH₂CH₂), 2.38 (t, J = 5.4 Hz, 2H, OCH₂CH₂).

74k was then prepared in a good yield following the aforementioned three-step procedure. 1H NMR (300 MHz, CDCl₃): δ 7.36–7.34 (m, 5H, Ph), 4.70 (d, J = 5.1 Hz, 2H, CH₂Ph), 4.61 (br, 1H, NH), 4.42 (s, 2H, OCH₂), 3.96 (t, J = 5.4 Hz, 2H, OCH₂CH₂), 2.79 (t, J = 5.4 Hz, 2H, OCH₂CH₂).

2-Methyl-1H-indole-4-carbonitrile (93p). *Step 1: 1-(Phenylsulfonyl)-1H-indole-4-carbonitrile (111p).* To a 0 °C solution of 1H-indole-4-carbonitrile (**111p**) (1.00 g, 7.0 mmol) in THF (20 mL) was added NaH (0.42 g, 10.5 mmol, 60%). The mixture was stirred for 5 min, and benzenesulfonyl chloride (1.49 g, 8.4 mmol) was then added at the same temperature. The reaction mixture was stirred at room temperature for an additional 30 min and then poured into a 0 °C saturated aqueous NH₄Cl solution (50 mL). The aqueous phase was separated and extracted with ethyl acetate (100 mL × 2); the combined organic layers were washed with water (50 mL) and brine (50 mL), dried over Na₂SO₄, and evaporated in vacuo. The residue was recrystallized (heptane, EtOAc) to give the intermediate (**112p**) (1.6 g, yield = 81%, purity = 99%) as a yellow solid. LRMS ($M + H^+$) m/z : calcd 283.1; found 283.0. 1H NMR (300 MHz, DMSO- d_6): δ 8.31 (d, J = 8.4 Hz, 1H), 8.15 (d, J = 3.9 Hz, 1H, 2-H of indole), 8.08–8.05 (m, 2H), 7.82–7.80 (m, 1H), 7.76–7.71 (m, 1H), 7.65–7.60 (m, 2H), 7.53 (t, J = 8.1 Hz, 1H), 7.00 (d, J = 3.9 Hz, 1H, 3-H of indole).

Step 2: 2-Methyl-1-(phenylsulfonyl)-1H-indole-4-carbonitrile (113p). To a –40 °C solution of the aforementioned indole intermediate (**112p**) (1.00 g, 3.5 mmol) in THF (30 mL) was slowly added *n*-BuLi (1.6 mL, 3.8 mmol, 2.4 M). The mixture was stirred for an additional 1 h, and then MeI (0.27 mL, 4.25 mmol) was added at the same temperature. The resulting mixture was then allowed to warm to room temperature and stirred for an extra 3 h. The mixture was poured into a 0 °C saturated aqueous NH₄Cl solution (100 mL). The aqueous phase was separated and extracted with EtOAc (100 mL × 2). The combined organic layers were washed with water (50 mL) and brine (50 mL × 2), dried over Na₂SO₄, and evaporated in vacuo. The residue was recrystallized (EtOAc, hexane) to give 2-methyl-1-(phenylsulfonyl)-1H-indole-4-carbonitrile (**113p**) (500 mg, yield = 47.6%, purity = 96%). LRMS ($M + H^+$) m/z : calcd 297.1; found 297.1. 1H NMR (300 MHz, DMSO- d_6): δ 8.37 (d, J = 8.4 Hz, 1H), 7.94 (d, J = 8.4 Hz, 2H), 7.74 (t, J = 6.9 Hz, 2H), 7.64–7.59 (m, 2H), 7.46 (t, J = 8.4 Hz, 1H), 6.82 (s, 1H, 3-H of indole), 2.68 (s, 3H, 2-Me).

Step 3: 2-Methyl-1H-indole-4-carbonitrile (93p). *Method A.* To a room temperature solution of the intermediate (**113p**) (18.5 g, 62.5 mmol) in ethanol (125 mL) was added aqueous sodium hydroxide solution (4 M, 47 mL, 188 mmol). Then the mixture was stirred at 40 °C for 3 h. The resulting solution was concentrated in vacuo and diluted with water (50 mL) and ethyl acetate (100 mL); the organic phase was separated, dried over sodium sulfate, and concentrated in vacuo. The residue was purified by column chromatography (silica gel, petroleum ether, ethyl acetate) to give the compound (**93p**) (6.7 g, yield = 69%). LRMS ($M + H^+$) m/z : calcd 157.1; found 157.1. 1H NMR (300 MHz, DMSO- d_6): δ 11.59 (s, 1H, NH), 7.61 (d, J = 8.1 Hz, 1H), 7.43 (d, J = 8.1 Hz, 1H), 7.13 (t, J = 8.1 Hz, 1H), 6.31 (s, 1H, 3-H of indole), 2.45 (s, 3H, 2-Me).

Step 3: 2-Methyl-1H-indole-4-carbonitrile (93p). *Method B.* To a room temperature solution of the intermediate (**93r**) (1.14 g, 5.4 mmol) in NMP (30 mL) were added Zn(CN)₂ (0.7 g, 6.0 mmol), Zn (75 mg, 1.1 mmol), dpfp (1.2 g, 2.2 mmol), and Pd₂(dba)₃ (1.0 g, 1.1 mmol). Then the resulting mixture was heated under an argon atmosphere at 120 °C for 18 h. It was cooled to room temperature and diluted with water (50 mL), then extracted with ethyl acetate (100 mL × 3). The combined organic layers were washed with water and brine, dried over anhydrous MgSO₄, and concentrated in vacuo. The residue was purified by flash chromatography (silica gel, petroleum ether, ethyl acetate) to give the desired compound (**93p**).

1-(4-(Benzylamino)-5,6,7,8-tetrahydropyrido[4,3-d]pyrimidin-2-yl)-2-methyl-1H-indole-4-carboxamide (65). *Step 1: N-tert-Butyl 4-(Benzylamino)-2-(4-cyano-2-methyl-1H-indol-1-yl)-7,8-dihydropyrido[4,3-d]pyrimidine-6(5H)-carboxylate.* To a room temperature solution of 2-methyl-1H-indole-4-carbonitrile (**93p**) (4.2 g, 26.7 mmol) and *N*-tert-butyl 4-(benzylamino)-2-chloro-7,8-dihydropyrido[4,3-d]pyrimidine-6(5H)-carboxylate (**74i**) (10 g, 26.7 mmol) in 1,4-dioxane (250 mL) was added cesium carbonate (13 g, 40 mmol). The mixture was degassed and filled with nitrogen three times. Pd₂(dba)₃ (3.66 g, 4 mmol) and X-Phos (1.9 g, 4 mmol) were then added. The resulting mixture was stirred at 100 °C for 12 h and cooled to room temperature. The volatiles were evaporated in vacuo, and the resulting residue was dissolved in methylene dichloride (500 mL), washed with water (50 mL) and brine (30 mL × 2), dried over Na₂SO₄, filtered, and evaporated in vacuo. The residue was purified by column chromatography (silica gel, petroleum ether, ethyl acetate) to give the *N*-tert-butyl 4-(benzylamino)-2-(4-cyano-2-methyl-1H-indol-1-yl)-7,8-dihydropyrido[4,3-d]pyrimidine-6(5H)-carboxylate (12.0 g, yield = 91%). LRMS ($M + H^+$) m/z : calcd 495.2; found 495.2.

Step 2: tert-Butyl 4-(Benzylamino)-2-(4-carbamoyl-2-methyl-1H-indol-1-yl)-7,8-dihydropyrido[4,3-d]pyrimidine-6(5H)-carboxylate (115). To a room temperature mixture of the aforementioned crude nitrile intermediate (150 mg, 0.30 mmol), PPh₃ (9.4 mg, 0.036 mmol), and Pd(OAc)₂ (6.7 mg, 0.03 mmol) in ethanol (4 mL) and water (0.5 mL) was added acetaldehyde oxime (35.4 mg, 0.60 mmol). The resulting mixture was refluxed for 2 h, cooled down to room temperature, and concentrated in vacuo. The residue was purified by flash chromatography (silica gel, petroleum ether, ethyl acetate) to afford crude *tert*-butyl 4-(benzylamino)-2-(4-carbamoyl-2-methyl-1H-indol-1-yl)-7,8-dihydropyrido[4,3-d]pyrimidine-6(5H)-carboxylate (**115**) (120 mg, yield = 78%). LRMS ($M + H^+$) m/z : calcd 513.2; found 513.2. 1H NMR (300 MHz, CDCl₃): δ 8.13 (d, J = 8.1 Hz, 1H, Ph of indole), 7.49 (d, J = 7.5 Hz, 1H, Ph of indole), 7.35–7.30 (m, 5H, Ph of NHBn), 7.09 (t, J = 7.8 Hz, 1H, Ph of indole), 6.83 (s, 1H, 3-H of indole), 4.74 (s, 2H, CH₂Ph), 4.34 (s, 2H, NCH₂), 3.76 (t, J = 5.7 Hz, 2H, NCH₂CH₂), 2.90 (t, J = 5.7 Hz, 2H, NCH₂CH₂), 2.63 (s, 3H, Me), 1.51 (s, 9H, C(CH₃)₃).

Step 3: 1-(4-(Benzylamino)-5,6,7,8-tetrahydropyrido[4,3-d]pyrimidin-2-yl)-2-methyl-1H-indole-4-carboxamide (65). To a 0 °C solution of the aforementioned crude Boc-protected intermediate (**115**) (11.5 g, 22.5 mmol) in methanol (500 mL) was bubbled hydrogen chloride slowly for 30 min. The resulting solution was concentrated in vacuo, the residue was dissolved in DCM (200 mL) and neutralized with ammonium hydroxide, the separated organic layer was dried over sodium sulfate, concentrated in vacuo, and purified by column chromatography (silica gel, DCM, methanol) to give the desired final product (**65**) (8.0 g, yield = 86%, purity = 99.8%) as solid. LRMS ($M + H^+$) m/z : calcd 413.2; found 413.1. 1H NMR (400 MHz, CD₃OD): δ 7.70 (d, J = 8.0 Hz, 1H, Ph of indole), 7.45 (d, J = 7.6 Hz, 1H, Ph of indole), 7.31–7.30 (m, 4H, Ph of NHBn), 7.26–7.22 (m, 1H, Ph of NHBn), 6.96 (t, J = 7.6 Hz, 1H, Ph of indole), 6.77 (s, 1H, 3-H of indole), 4.71 (s, 2H, CH₂Ph), 3.78 (s, 2H, NCH₂), 3.16 (t, J = 6.0 Hz, 2H, NCH₂CH₂), 2.77 (t, J = 6.0 Hz, 2H, NCH₂CH₂), 2.43 (s, 3H, Me). ^{13}C NMR (400 MHz, CD₃OD): δ 174.10, 161.77, 161.61, 156.15, 140.97, 140.36, 138.96, 129.58, 128.59, 127.95, 127.85, 125.79, 122.04, 121.87, 117.37, 110.11, 105.31, 45.29, 43.40, 42.87, 31.89, 15.51.

1-(4-(Benzylamino)-5,6,7,8-tetrahydroquinazolin-2-yl)-2-methyl-1H-indole-4-carboxamide (69). A two-step procedure similar to the aforementioned was followed to couple intermediates **74h** and **93p** followed by oxidation using Pd(OAc)₂ catalyzed oxidation with acetaldehyde oxime to yield the desired molecule (**69**) (purity = 98%). LRMS ($M + H^+$) m/z : calcd 412.2; found 412.2. 1H NMR (400 MHz, CD₃OD): δ 7.63 (d, J = 8.4 Hz, 1H, Ph of indole), 7.46 (d, J = 7.6 Hz, 1H, Ph of indole), 7.44–7.31 (m, 5H, Ph of Bn), 6.96 (t, J = 7.6 Hz, 1H, Ph of indole), 6.76 (s, 1H, 3-H of indole), 4.72 (s, 2H, CH₂Ph), 2.74 (t, J = 5.6 Hz, 2H, CH₂), 2.54 (t, J = 6.0 Hz, 2H, CH₂), 2.42 (s, 3H, Me), 1.94–1.92 (m, 4H, (CH₂)₂).

1-[4-(Benzylamino)-5H,7H,8H-pyrano[4,3-d]pyrimidin-2-yl]-2-methyl-1H-indole-4-carboxamide (71). A two-step procedure

similar to the aforementioned was followed to couple intermediate **74k** with intermediate **93p** and then Pd(OAc)₂ catalyzed oxidation with acetaldehyde oxime was used to yield the desired molecule (**71**) (purity = 98.5%). LRMS (M + H⁺) *m/z*: calcd 414.2; found 414.1. ¹H NMR (400 MHz, CD₃OD): δ 7.73 (d, *J* = 8.4 Hz, 1H, Ph), 7.46 (d, *J* = 7.6 Hz, 1H, Ph), 7.34–7.29 (m, 4H, Ph), 7.27–7.24 (m, 1H, Ph), 6.97 (t, *J* = 7.6 Hz, 1H, Ph), 6.78 (s, 1H, 3-H of indole), 4.71 (s, 2H, CH₂Ph), 4.64 (s, 2H, OCH₂), 4.05 (t, *J* = 5.6 Hz, 2H, OCH₂CH₂), 2.82 (t, *J* = 5.6 Hz, 2H, OCH₂CH₂), 2.45 (s, 3H, Me). ¹³CNMR (400 MHz, CD₃OD): δ 174.06, 160.71, 160.45, 156.45, 140.82, 140.42, 138.91, 129.58, 128.62, 127.95, 127.83, 125.75, 122.06, 121.91, 117.57, 109.72, 105.48, 65.68, 64.08, 45.24, 31.78, 15.72.

Biology. The ATPase assay is performed according to the following protocol: compounds were diluted in DMSO with a 3-fold 10-point serial dilution starting at 10 μM. The assay was done in a 384-well plate with each row as a single dilution series with duplicate of each compound concentration point. In 5 μL total volume, 20 nM p97 hexameric enzyme and 20 μM ATP were added to start the reaction. The plate was sealed and incubated at 37 °C for 15 min after mixing thoroughly in an orbital shaker. Compound dilution, ATP and enzymes addition were conducted with automated liquid handling using the Freedom Evo (Tecan Systems Inc., San Jose, CA). ADP Glo reagents 1 and 2 were added according to the manufacturer's protocol (Promega, Madison, WI). The luminescence was measured by Envision plate reader as the end point of the reaction. The IC₅₀ of each compound was derived by fitting the luminescence values to a four-parameter sigmoidal curve.³⁶

A549 and other tumor cell lines were cultured according to ATCC guidelines. Cells were cultured in black or white, clear-bottomed, tissue culture-treated 384-well plates. Cells were treated with 10-point dose titration of the compound in well duplicates. After a 72 h treatment, CellTiter-Glo (Promega, Madison, WI) was added to the white plates to measure cell viability. Luminescence values were fit to a four-parameter sigmoidal curve to determine IC₅₀ concentrations. For the cell-based PD assays, paraformaldehyde (4% final concentration) was added to black plates for 5 min following a 6 h treatment with compound. Cells were then washed in PBS and processed for immunofluorescence. Cells were blocked in 1× phosphate buffered saline (PBS) with 1% BSA, 0.3% Triton-X100, and Hoechst (1:10 000) for 1 h and then incubated in primary antibodies at 4 °C for 16 h. Primary antibodies used are as follows: anti-Lys48 ubiquitin at 1:20 000 (05-1307, Millipore, Billerica, MA), anti-CHOP at 1:2000 (SC-7351, Santa Cruz, Biotechnology Inc., Santa Cruz, CA), and p62/SQSTM1 at 1:2000 (SC-28359, Santa Cruz, Biotechnology Inc., Santa Cruz, CA). Cells were washed 3 times in PBS, and secondary antibodies were added for 2 h at 25 °C. Cells were washed 4 times in PBS and imaged with an automated wide field fluorescence microscope. Automated image analysis was written in Matlab (Mathworks, Natick, MA). Cellular intensities for each marker were measured. Fluorescence intensity values were fit to a four-parameter sigmoidal curve to determine IC₅₀ concentrations for each marker.

All mice were maintained in the Cleave Biosciences animal vivarium, and all in vivo experiments were performed in compliance with applicable regulations and institutional guidelines and had been approved by the Cleave Biosciences IACUC.

■ ASSOCIATED CONTENT

■ Supporting Information

The Supporting Information is available free of charge on the ACS Publications website at DOI: 10.1021/acs.jmedchem.5b01346.

Antitumor response induced by oral administration of compound **35**; crystal structure information on **71**; synthetic methods for compounds **12–14**, **32**, **35**, **40**, **47–49**, and **64**; purity and spectral data of compounds **9–23**, **27–31**, **33**, **34**, **36–38**, **41–46**, **50–63**, **66–68**, **70**, **72** (PDF)

Molecular formula strings covering 7–72 except **39** (CSV)

■ AUTHOR INFORMATION

Corresponding Author

*Phone: 1-650-443-3013. Fax: 1-877-258-4146. E-mail: hjzhou@cleavebio.com.

Notes

The authors declare no competing financial interest.

■ ACKNOWLEDGMENTS

We thank Professor Ray Deshaies at California Institute of Technology, Assistant Professor Tsui-Fen Chou at Harbor-ULCA, and Dr. Frank J. Schoenen and Dr. Kelin Li at University of Kansas for sharing their SAR knowledge on discovery of ML240. Special thanks are extended to Dr. Ethan Emberly, Victoria Pickering, and Alina Boltunova for their contribution to the early stage of the project. We acknowledge Dr. Jian Lu Chen, Jenny Pham, and Jean Zhang for their contributions to this project as well. We are grateful to the chemists led by Dr. Changjia Zhao at BioDuro (PPD) for their support in synthesis. We are thankful to Pharmorphix for growing CB-5083 dihydrate crystals and analyzing the X-ray structure, and we are thankful to ActivX for profiling our compounds' p97 ATP binding sites. This program was fully funded by Cleave Biosciences Inc.

■ ABBREVIATIONS USED

VCP, valosin-containing protein; CDC48, cell division cycle 48; AAA, ATPase associated with diverse cellular activity; UPS, ubiquitin–proteasome system; ER, endoplasmic reticulum; ERAD, endoplasmic reticulum-associated degradation; UPR, unfolded protein response; HTS, high-throughput screening; SAR, structure and activity relationship; p97i, p97 inhibition; CTG, CellTiter-Glo; CHOP, CCAAT/enhancer-binding homologous protein; p62, sequestosome 1; PARP, poly ADP-ribose polymerase; SGF, simulated gastric fluid; SIF, simulated intestinal fluid; MLM, mice liver microsome; cLogP, calculated log *P*; PSA, molecular polar surface area; LipE, lipophilic efficiency; iv, intravenous administration; po, oral administration; PK, pharmacokinetics; PD, pharmacodynamics; *F*, absolute bioavailability in %

■ REFERENCES

- (1) (a) Koller, K. J.; Brownstein, M. J. Use of a cDNA clone to identify a supposed precursor protein containing valosin. *Nature* **1987**, 325 (6104), 542–545. (b) Frohlich, K. U.; Fries, H. W.; Rudiger, M.; Erdmann, R.; Botstein, D.; Mecke, D. Yeast cell cycle protein CDC48p shows full-length homology to the mammalian protein VCP and is a member of a protein family involved in secretion, peroxisome formation, and gene expression. *J. Cell Biol.* **1991**, 114 (3), 443–453.
- (2) Buchberger, A.; Schindelin, H.; Hänzelmann, P. Control of p97 function by cofactor binding. *FEBS Lett.* **2015**, 589 (19, Part A), 2578–2589.
- (3) Meyer, H.; Bug, M.; Bremer, S. Emerging functions of the VCP/p97 AAA-ATPase in the ubiquitin system. *Nat. Cell Biol.* **2012**, 14 (2), 117–123.
- (4) Chou, T. F.; Deshaies, R. J. Development of p97 AAA ATPase inhibitors. *Autophagy* **2011**, 7 (9), 1091–1092.
- (5) Dargemont, C.; Ossareh-Nazari, B. Cdc48/p97, a key actor in the interplay between autophagy and ubiquitin/proteasome catabolic pathways. *Biochim. Biophys. Acta, Mol. Cell Res.* **2012**, 1823 (1), 138–144.

- (6) Dantuma, N. P.; Acs, K.; Luijsterburg, M. S. Should I stay or should I go: VCP/p97-mediated chromatin extraction in the DNA damage response. *Exp. Cell Res.* **2014**, *329* (1), 9–17.
- (7) Orme, C. M.; Bogan, J. S. The ubiquitin regulatory X (UBX) domain-containing protein TUG regulates the p97 ATPase and resides at the endoplasmic reticulum-golgi intermediate compartment. *J. Biol. Chem.* **2012**, *287* (9), 6679–6692.
- (8) DeLaBarre, B.; Brunger, A. T. Complete structure of p97/valosin-containing protein reveals communication between nucleotide domains. *Nat. Struct. Biol.* **2003**, *10* (10), 856–863.
- (9) Wang, Q.; Song, C.; Li, C. C. Molecular perspectives on p97-VCP: progress in understanding its structure and diverse biological functions. *J. Struct. Biol.* **2004**, *146* (1–2), 44–57.
- (10) Song, C.; Wang, Q.; Li, C. C. ATPase activity of p97-valosin-containing protein (VCP). D2 mediates the major enzyme activity, and D1 contributes to the heat-induced activity. *J. Biol. Chem.* **2003**, *278* (6), 3648–3655.
- (11) Raasi, S.; Wolf, D. H. Ubiquitin receptors and ERAD: a network of pathways to the proteasome. *Semin. Cell Dev. Biol.* **2007**, *18* (6), 780–791.
- (12) Wójcik, C.; Rowicka, M.; Kudlicki, A.; Nowis, D.; McConnell, E.; Kujawa, M.; DeMartino, G. N. Valosin-containing protein (p97) is a regulator of endoplasmic reticulum stress and of the degradation of N-end rule and ubiquitin-fusion degradation pathway substrates in mammalian cells. *Mol. Biol. Cell* **2006**, *17* (11), 4606–4618.
- (13) (a) Wustrow, D.; Zhou, H.-J.; Rolfe, M., Chapter fourteen—Inhibition of ubiquitin proteasome system enzymes for anticancer therapy. In *Annu. Rep. Med. Chem.*; Manoj, C. D., Ed.; Academic Press: London, 2013; Vol. 48, pp 205–225. (b) Deshaies, R. J. Proteotoxic crisis, the ubiquitin-proteasome system, and cancer therapy. *BMC Biol.* **2014**, *12*, 94. (c) Chapman, E.; Maksim, N.; de la Cruz, F.; La Clair, J. J. Inhibitors of the AAA+ chaperone p97. *Molecules* **2015**, *20* (2), 3027–3049.
- (14) Bursavich, M. G.; Parker, D. P.; Willardsen, J. A.; Gao, Z. H.; Davis, T.; Ostanin, K.; Robinson, R.; Peterson, A.; Cimbara, D. M.; Zhu, J. F.; Richards, B. 2-Anilino-4-aryl-1,3-thiazole inhibitors of valosin-containing protein (VCP or p97). *Bioorg. Med. Chem. Lett.* **2010**, *20* (5), 1677–1679.
- (15) Magnaghi, P.; D'Alessio, R.; Valsasina, B.; Avanzi, N.; Rizzi, S.; Asa, D.; Gasparri, F.; Cozzi, L.; Cucchi, U.; Orrenius, C.; Polucci, P.; Ballinari, D.; Perrera, C.; Leone, A.; Cervi, G.; Casale, E.; Xiao, Y.; Wong, C.; Anderson, D. J.; Galvani, A.; Donati, D.; O'Brien, T.; Jackson, P. K.; Isacchi, A. Covalent and allosteric inhibitors of the ATPase VCP/p97 induce cancer cell death. *Nat. Chem. Biol.* **2013**, *9* (9), 548–556.
- (16) Polucci, P.; Magnaghi, P.; Angiolini, M.; Asa, D.; Avanzi, N.; Badari, A.; Bertrand, J. A.; Casale, E.; Cauteruccio, S.; Cirila, A.; Cozzi, L.; Galvani, A.; Jackson, P. K.; Liu, Y.; Magnuson, S.; Malgesini, B.; Nuvoloni, S.; Orrenius, C.; Riccardi Sirtori, F.; Riceputi, L.; Rizzi, S.; Trucchi, B.; O'Brien, T.; Isacchi, A.; Donati, D.; D'Alessio, R. Alkylsulfanyl-1,2,4-triazoles, a new class of allosteric valosine containing protein inhibitors. Synthesis and structure-activity relationships. *J. Med. Chem.* **2013**, *56* (2), 437–450.
- (17) Cervi, G.; Magnaghi, P.; Asa, D.; Avanzi, N.; Badari, A.; Borghi, D.; Caruso, M.; Cirila, A.; Cozzi, L.; Felder, E.; Galvani, A.; Gasparri, F.; Lomolino, A.; Magnuson, S.; Malgesini, B.; Motto, I.; Pasi, M.; Rizzi, S.; Salom, B.; Sorrentino, G.; Troiani, S.; Valsasina, B.; O'Brien, T.; Isacchi, A.; Donati, D.; D'Alessio, R. Discovery of 2-(cyclohexylmethylamino)pyrimidines as a new class of reversible valosine containing protein inhibitors. *J. Med. Chem.* **2014**, *57* (24), 10443–10454.
- (18) Chou, T. F.; Brown, S. J.; Minond, D.; Nordin, B. E.; Li, K.; Jones, A. C.; Chase, P.; Porubsky, P. R.; Stoltz, B. M.; Schoenen, F. J.; Patricelli, M. P.; Hodder, P.; Rosen, H.; Deshaies, R. J. Reversible inhibitor of p97, DBE-Q, impairs both ubiquitin-dependent and autophagic protein clearance pathways. *Proc. Natl. Acad. Sci. U. S. A.* **2011**, *108* (12), 4834–4839.
- (19) Chou, T. F.; Li, K.; Frankowski, K. J.; Schoenen, F. J.; Deshaies, R. J. Structure-activity relationship study reveals ML240 and ML241 as potent and selective inhibitors of p97 ATPase. *ChemMedChem* **2013**, *8* (2), 297–312.
- (20) Chou, T. F.; Bulfer, S. L.; Wehl, C. C.; Li, K.; Lis, L. G.; Walters, M. A.; Schoenen, F. J.; Lin, H. J.; Deshaies, R. J.; Arkin, M. R. Specific inhibition of p97/VCP ATPase and kinetic analysis demonstrate interaction between D1 and D2 ATPase domains. *J. Mol. Biol.* **2014**, *426* (15), 2886–2899.
- (21) Kikelj, D. Product class 13: quinazolines. *Sci. Synth.* **2004**, *16*, 573–749.
- (22) Henteman, M. F.; Scott, W.; Wood, J.; Johnson, J.; Redman, A.; Bullion, A.-M.; Guernon, L. Preparation of sulfonyldihydroimidazoquinazoline derivatives for use as PIK3 inhibitors. WO2009091550A2, 2009.
- (23) Kuhn, B.; Mohr, P.; Stahl, M. Intramolecular hydrogen bonding in medicinal chemistry. *J. Med. Chem.* **2010**, *53* (6), 2601–2611.
- (24) Hamley, P.; Tinker, A. C. 1,2-Diaminobenzimidazoles: selective inhibitors of nitric oxide synthase derived from aminoguanidine. *Bioorg. Med. Chem. Lett.* **1995**, *5* (15), 1573–1576.
- (25) Ohno, K.; Ishida, W.; Kamata, K.; Oda, K.; Machida, M. Synthesis of 2-dimethylaminobenzazoles via a guanidine intermediate. Reaction of 2-substituted aniline derivatives with 2-chloro-1,1,3,3-tetramethyl-formamminium chloride. *Heterocycles* **2003**, *59* (1), 317–322.
- (26) Little, T. L.; Webber, S. E. A simple and practical synthesis of 2-aminoimidazoles. *J. Org. Chem.* **1994**, *59* (24), 7299–7305.
- (27) Ple, P.; Jung, F. H. Preparation of quinazoline derivatives for use in treatment of cell proliferative disorders or disease assocd. with angiogenesis and/or vascular permeability. WO2006040520A1, 2006.
- (28) Odingo, J.; O'Malley, T.; Kesicki, E. A.; Alling, T.; Bailey, M. A.; Early, J.; Ollinger, J.; Dalai, S.; Kumar, N.; Singh, R. V.; Hipskind, P. A.; Cramer, J. W.; Ioerger, T.; Sacchettini, J.; Vickers, R.; Parish, T. Synthesis and evaluation of the 2,4-diaminoquinazoline series as anti-tubercular agents. *Bioorg. Med. Chem.* **2014**, *22* (24), 6965–6979.
- (29) Childress, S. J.; McKee, R. L. Thiazolopyrimidines. *J. Am. Chem. Soc.* **1951**, *73* (8), 3862–3864.
- (30) Dowd, P.; Choi, S.-C. Free radical ring-expansion leading to novel six- and seven-membered heterocycles. *Tetrahedron* **1991**, *47* (27), 4847–4860.
- (31) Koehler, M. F. T.; Bergeron, P.; Blackwood, E.; Bowman, K. K.; Chen, Y.-H.; Deshmukh, G.; Ding, X.; Epler, J.; Lau, K.; Lee, L.; Liu, L.; Ly, C.; Malek, S.; Nonomiya, J.; Oeh, J.; Ortwine, D. F.; Sampath, D.; Sideris, S.; Trinh, L.; Truong, T.; Wu, J.; Pei, Z.; Lyssikatos, J. P. Potent, selective, and orally bioavailable inhibitors of the mammalian target of rapamycin kinase domain exhibiting single agent antiproliferative activity. *J. Med. Chem.* **2012**, *55* (24), 10958–10971.
- (32) Estep, K. G.; Fliri, A. F. J.; O'Donnell, C. J. Arylheterocycle-sulfonamide derivatives as AMPA modulators and their preparations, pharmaceutical compositions and use in the treatment of diseases. WO2008120093A1, 2008.
- (33) Shultz, M. D.; Cao, X.; Chen, C. H.; Cho, Y. S.; Davis, N. R.; Eckman, J.; Fan, J.; Fekete, A.; Firestone, B.; Flynn, J.; Green, J.; Growney, J. D.; Holmqvist, M.; Hsu, M.; Jansson, D.; Jiang, L.; Kwon, P.; Liu, G.; Lombardo, F.; Lu, Q.; Majumdar, D.; Meta, C.; Perez, L.; Pu, M.; Ramsey, T.; Remiszewski, S.; Skolnik, S.; Traebert, M.; Urban, L.; Uttamsingh, V.; Wang, P.; Whitebread, S.; Whitehead, L.; Yan-Neale, Y.; Yao, Y.-M.; Zhou, L.; Atadja, P. Optimization of the in vitro cardiac safety of hydroxamate-based histone deacetylase inhibitors. *J. Med. Chem.* **2011**, *54* (13), 4752–4772.
- (34) Zhou, H.-J.; Parlati, F.; Wustrow, D. Preparation of fused pyrimidines as inhibitors of p97 complex. WO2014015291A1, 2014.
- (35) Hesse, S.; Perspicace, E.; Kirsch, G. Microwave-assisted synthesis of 2-aminothiophene-3-carboxylic acid derivatives, 3H-thieno[2,3-d]pyrimidin-4-one and 4-chlorothieno[2,3-d]pyrimidine. *Tetrahedron Lett.* **2007**, *48* (30), 5261–5264.
- (36) Anderson, D. J.; Le Moigne, R.; Djakovic, S.; Kumar, B.; Rice, J.; Wong, S.; Wang, J.; Yao, B.; Valle, E.; Soly, S. K. V.; Madriaga, A.; Soriano, F.; Menon, M.-K.; Kampmann, M.; Chen, Y.; Weissman, J. S.; Aftab, B.; Yakes, F. M.; Shawver, L.; Zhou, H. – J.; Wustrow, D.; Rolfe, M. Targeting the AAA ATPase, p97, as a novel approach to treat

cancer through disruption of protein homeostasis. *Cancer Cell* **2015**, 28 (5), 653–665.

(37) Yoshida, H.; Okada, T.; Haze, K.; Yanagi, H.; Yura, T.; Negishi, M.; Mori, K. ATF6 activated by proteolysis binds in the presence of NF-Y (CBF) directly to the cis-acting element responsible for the mammalian unfolded protein response. *Mol. Cell. Biol.* **2000**, 20 (18), 6755–6767.

(38) Wang, Y.; Serradell, N.; Bolos, J.; Rosa, E. YM-155: apoptosis inducer survivin expression inhibitor oncolytic. *Drugs Future* **2007**, 32 (10), 879–882.

(39) Bjorkoy, G.; Lamark, T.; Johansen, T. p62/SQSTM1: a missing link between protein aggregates and the autophagy machinery. *Autophagy* **2006**, 2 (2), 138–139.

(40) (a) Ryckmans, T.; Edwards, M. P.; Horne, V. A.; Correia, A. M.; Owen, D. R.; Thompson, L. R.; Tran, I.; Tutt, M. F.; Young, T. Rapid assessment of a novel series of selective CB(2) agonists using parallel synthesis protocols: a lipophilic efficiency (LipE) analysis. *Bioorg. Med. Chem. Lett.* **2009**, 19 (15), 4406–4409. (b) Leeson, P. D.; Springthorpe, B. The influence of drug-like concepts on decision-making in medicinal chemistry. *Nat. Rev. Drug Discovery* **2007**, 6 (11), 881–890.

(41) Shultz, M. D. Setting expectations in molecular optimizations: strengths and limitations of commonly used composite parameters. *Bioorg. Med. Chem. Lett.* **2013**, 23 (21), 5980–5991.